

# Vertical axis rotation in the Bolivian orocline, South America

## 1. Paleomagnetic analysis of Cretaceous and Cenozoic rocks

Simon Lamb

Department of Earth Sciences, University of Oxford, Oxford, England, UK

**Abstract.** The results of a paleomagnetic study are reported for 45 new sites or localities in the central Andes of Bolivia and northern Chile (17°S–23°S), South America, in intrusive, volcanic and sedimentary rocks, ranging in age between ~7 and ~80 Ma. These outcrop across the width of the northern and southern limbs of the Bolivian orocline, from the sub-Andean zone in the east to the volcanic arc in the west. For most localities a mean primary magnetization has been identified which is assumed to reflect a geocentric axial dipole field. A comparison of directions of magnetizations with those predicted by the relevant paleomagnetic reference poles for stable South America reveals declination anomalies which are interpreted in terms of the rotation about a local vertical axis of rigid crustal blocks (hundreds of meters to tens of kilometers across), relative to stable South America. These data, when combined with previous paleomagnetic studies of Upper Cretaceous and Cenozoic rocks, show a pattern of vertical axis rotations which defines three regional domains, extending across the width of the Bolivian Andes. The differences between the various domains are best seen in rocks in the age range ~20 to 80 Ma; younger rocks acquired a primary magnetization at later stages in the rotation history. For rocks older than 20 Ma, crustal blocks in domain 1, on the northern flank of the Bolivian orocline, have undergone an anticlockwise rotation about a vertical axis in the range ~8 to ~33°, with a geometric mean of ~22°; blocks from domain 2 immediately south of the main oroclinal bend have rotated between ~19° anticlockwise and ~40° clockwise, with a geometric mean of ~8° clockwise. Even farther south, in domain 3b, blocks have rotated between ~3° and ~57° clockwise, with a geometric mean of 37°. A localised area (domain 3b), in which blocks have undergone ~32° clockwise rotation in the last ~65 Myr, lies within the southeastern part of domain 1. The northern boundary of domain 1 and the southern boundary of domain 3a are as yet not well defined. The amount and timing of Cenozoic vertical axis rotation vary across the width of the Andes, and are interpreted to record both regional bending of both limbs of the Bolivian orocline and small block rotation in zones of distributed sinistral or dextral shear during three stages in the Cenozoic: (1) ~45 to ~25 Ma, (2) ~25 to ~10 Ma, (3) ~10 Ma to 0. Bending of the Bolivian Andes during the last ~25 Myr was accommodated, relative to stable South America, by gradients of shortening along the eastern margin of the Andes, particularly in the sub-Andean zone.

### 1. Introduction

Sinuous chains of mountains, often with abrupt changes in trend, form prominent features of the continents. Many examples can be found in the varying trend of the Alpine-Himalayan zone, or the Andes on the western margin of South America. It is generally unclear whether these bends or oroclines are primary features, which have existed since the inception of deformation in the mountain belt, or whether they have developed during the evolution of deformation. In either case, at some fundamental level they reflect spatial variations in the forces that drive continental deformation, the rheology of the continental lithosphere, and the resulting bulk strain. Thus unravelling the evolution of oroclines has the potential to improve our understanding of the dynamics of continental deformation.

In this paper, rigid body rotations about vertical axes, determined from paleomagnetic measurements, are used to better define the Cenozoic tectonic evolution of the Bolivian Andes. Here,

there is a pronounced change in the topographic trend, referred to as the Bolivian orocline. This paper presents new paleomagnetic data, covering a large part of the Bolivian Andes, between 6°S and 23°S and 64°W and 69°W, which, combined with those determined in previous studies, are used to constrain the timing and distribution of rotation about a vertical axis of crustal blocks. *Lamb* [this issue] investigates the kinematic consequences and dynamical controls of these rotations in the context of the rheology of Andean lithosphere.

### 2. Geological Setting of the Central Andes

The central Andes, which are part of the second largest mountainous region on Earth, offer many advantages as a place to study convergent continental deformation in large mountain belts. Widespread diffuse shallow seismicity shows that they are actively deforming. They have a fairly well understood long-term evolution; a wealth of geological data can be obtained from the thick and extensive sedimentary basins that formed both before and during mountain building [*Sempere et al.*, 1990; *Lamb et al.*, 1997; *Lamb and Hoke*, 1997; *Allmendinger et al.*, 1997]. Finally, unlike other regions of convergent continental deformation, such

Copyright 2001 by the American Geophysical Union.

Paper number 2001JB900012.  
0148-0227/01/2001JB900012\$09 00

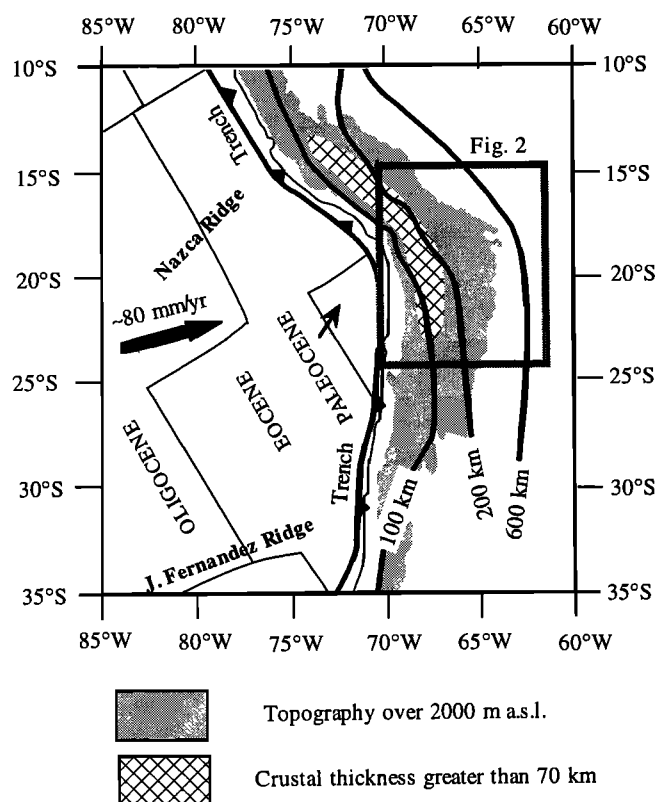


**Figure 1.** Map of the western margin of South America between 10°S and 35°S. The oceanic Nazca plate is being subducted beneath the continental South American plate along the Peru-Chile trench at  $\sim 80$  mm/yr toward  $\sim 075^\circ$  (NUVEL-1A [DeMets et al., 1994]). Also illustrated are region with topography above 2000 m in the central Andes, contours to the Benioff zone [Dewey and Lamb, 1992], region with crust  $>70$  km thick [after James, 1971], and the age structure of the oceanic Nazca plate. Box shows outline of map in Figure 2.

as the Himalayas and Tibet, they are very accessible, situated on the western margin of South America (Figure 1). Here, the Nazca oceanic plate (and former oceanic plates) is being subducted beneath the continental lithosphere of the South American plate at  $\sim 80$  mm yr $^{-1}$  in a roughly ENE direction (Figure 1, NUVEL-1A [DeMets et al., 1994]). The finite relative plate motions are well known for the past 68 Myr [Pardo-Casas and Molnar, 1987].

At the latitudes of Bolivia, a well-defined Benioff zone dips at  $\sim 30^\circ$  beneath the Andes, and there is an active volcanic arc, which follows the western margin of the high Andes. The region can be conveniently divided into several physiographic and geological provinces (Figures 2 and 3). The high central plateau of the Altiplano, which is at an average elevation of  $\sim 3.8$  km and up to 200 km wide, is bounded to the west by the volcanic arc (Western Cordillera) and forearc in northern Chile and southern Peru and to the east by the rugged Eastern Cordillera. The Eastern Cordillera locally reaches elevations up to 6.5 km and becomes progressively lower in the sub-Andean zone. Earthquakes show that the eastern margin of the sub-Andean zone is the locus of active deformation, accommodating underthrusting of the foreland region, comprising the Brazilian Shield, beneath the Andes in a thin-skinned fold and thrust belt.

Numerous paleomagnetic studies in the central Andes have determined Cenozoic vertical axis rotations of crustal blocks on both limbs of the Bolivian orocline [Heki et al., 1985; Kono et al.,

1985; Beck, 1988; McFadden et al., 1990, 1993, 1995; Roperch and Carlier, 1992; Hartley et al., 1992; Roperch et al., 1993, 1996, 1999, 2000; Butler et al., 1995; Somoza et al., 1996, 1999; Coutand et al., 1999]. Despite this work, no clear and definitive picture has emerged of the temporal and spatial evolution of rotational strain, though a number of models have been proposed (reviewed by Randall [1998] and Beck [1998]) that relate the observed rotation to (1) oroclinal bending; (2) distributed shear related to the margin-parallel component of relative plate motion; or (3) some combination of 1 and 2. This study reports the results of paleomagnetic sampling at 45 new sites or localities in sedimentary, intrusive, and volcanic rocks, ranging in age between  $\sim 7$  and  $\sim 80$  Ma. Vertical axis rotations have been determined for localities along the length of the Bolivian Andes, on both limbs of the Bolivian orocline, and also across the width from the sub-Andean zone to the volcanic arc (Figures 2-7).

### 3. Paleomagnetic Results

#### 3.1. Sampling and Analytical Procedures

Unweathered rock cores were taken from sites using either a portable petroleum-engined drill with a diamond-tipped barrel (internal diameter 25 mm) or, in some cases, orientated blocks. All sites contained clear evidence of bedding and way up and a lack of internal deformation. Samples from sandstones and siltstones were collected from water-saturated outcrops close to stream level and were wrapped in cling film in order to prevent drying out, which experience has shown to produce a strong viscous remanence. The sampling strategy for sedimentary rocks at any particular locality was designed to capture the Earth's magnetic field at as many sites as possible over time spans in excess of 10,000 years in order to adequately average the effects of paleosecular variation (see discussion below).

The magnetization from unaltered specimens (one to three specimens cut from individual samples (cores)) was measured on cryogenic and Molspin magnetometers at the Department of Earth Sciences at Oxford. All samples were subjected to stepwise thermal, and sometimes alternating field, demagnetization until usually no measurable signal remained (typically  $<1\%$  of the initial intensity). Components of the specimen magnetic field were analyzed with Zijderveld [1967] demagnetization plots, using the least squares algorithms in the IAPD (Interactive Analysis of Paleomagnetic Data) software [Torsvik et al., 1996] to determine best fitting magnetic vectors. In most cases, bulk susceptibility was also measured after each demagnetization step to monitor the growth of magnetic minerals during heating. In addition, induced remanence magnetization (IRM) studies were carried out on selected specimens to investigate the magnetic carriers.

The specimens, samples, and their sites, localities, and structural and stratigraphic context, as well as demagnetization characteristics, are described below and summarized in Figures 3-14 and Tables 1-5. Sampling localities are given two- to five-letter labels in capitals, while samples and specimens from individual sites at a locality are given an alphanumeric code.

#### 3.2. Upper Cretaceous to Paleocene Limestones

A sequence of Cretaceous to Paleocene marine and lacustrine sandstones, shales and limestones outcrops extensively in the Altiplano and Eastern Cordillera of the Bolivian Andes. Fossil evidence (summarized in Riccardi [1988]) shows that most of the Cretaceous in Bolivia is Cenomanian and younger. In the lower part of the Cretaceous sequence the distinctive gray limestone se-

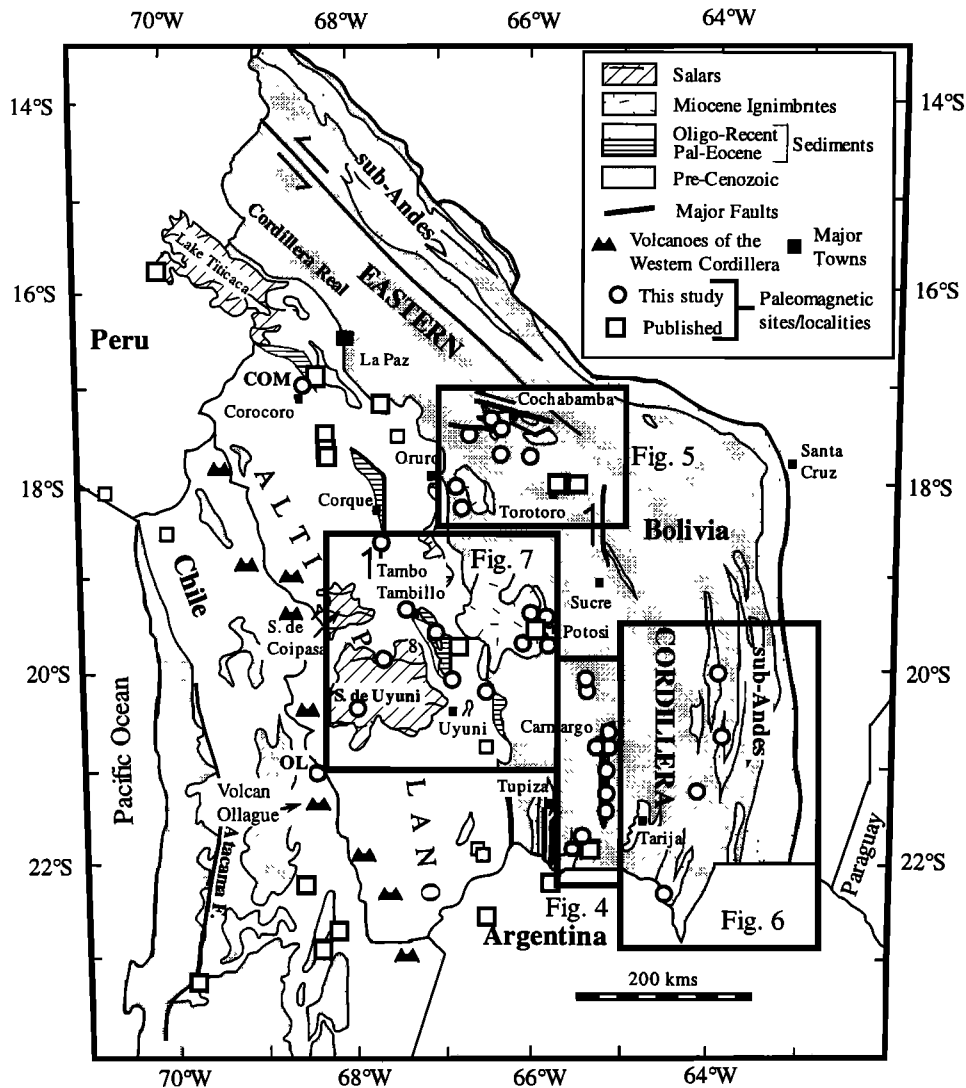


**Figure 2.** Geological map of the Bolivian Andes, simplified from the published scale 1:1,000,000 geological map of Bolivia (modified from *Bolivian Geological Survey (GEOBOL) and Yacimientos Petroliferos Fiscales Bolivianos (YPFB)* [1978]). Paleomagnetic sites or localities, analyzed in this and previous published studies, are shown (see Table 6 and references therein). Boxes show the regions illustrated in Figures 4-7. The pronounced bend in structural trend and topography at  $\sim 18^\circ\text{S}$  is referred to as the Bolivian orocline. The Bolivian Andes can be divided into a series of physiographic provinces, which, from east to west, consist of (1) the Amazon and Chaco basins, east of the Andes, which form a stable foreland generally at altitudes of 100's m above sea level; (2) sub-Andes, generally at altitudes up to 2 km; (3) rugged Eastern Cordillera, mainly consisting of Lower Paleozoic flysch-like sequences, generally at altitudes 3-4.5 km; (4) Altiplano, which forms a high plateau region of subdued relief at elevations of  $\sim 4$  km, underlain by thick Cenozoic red bed sequences; and (5) the volcanic arc on the western margin of the Altiplano, referred to as the Western Cordillera, consisting of spaced andesitic cones and small dacitic domes, rising nearly 2 km above the general level of the surrounding regions. West of the volcanic arc, the Andes slope down toward the forearc and Pacific Ocean.

quences of the Miraflores Formation were deposited in a marine environment. In the Maastrichtian to Paleocene the basin was at its widest. A laterally extensive marine and lacustrine sequence of this age (Figures 3-5, El Molino and Santa Lucia Formations [Gayet et al., 1991; Rouchy et al., 1993; Sempere et al., 1997]), up to several hundred meters thick, rests directly on the Paleozoic basement. The lateral continuity and extensive outcrop of these strata demonstrate that most of the Bolivian Andes was a region of very subdued topography at or near sea level at this time. The subsequent deformation of these rocks records the total finite Cenozoic strain that has created the present topography in the central Andes.

In detail, the Upper Cretaceous to Paleocene sequence consists of medium sandstones, purple and gray shales, and well-bedded pink or gray oolitic, stromatoporoid, and micritic limestones. These were sampled at a number of locations over a stratigraphic thickness of a few meters to several tens of meters. The limestones are folded, with fold limb dips ranging between subvertical and subhorizontal. In the southern part of the Eastern Cordillera, Upper Cretaceous to Paleocene limestones outcrop extensively, extending along strike for nearly 200 km in two regional fold structures, referred to as the Otavi and Camargo synclines (Figures 4, 8a, and b). Here, it was possible to sample both limbs of the folds.

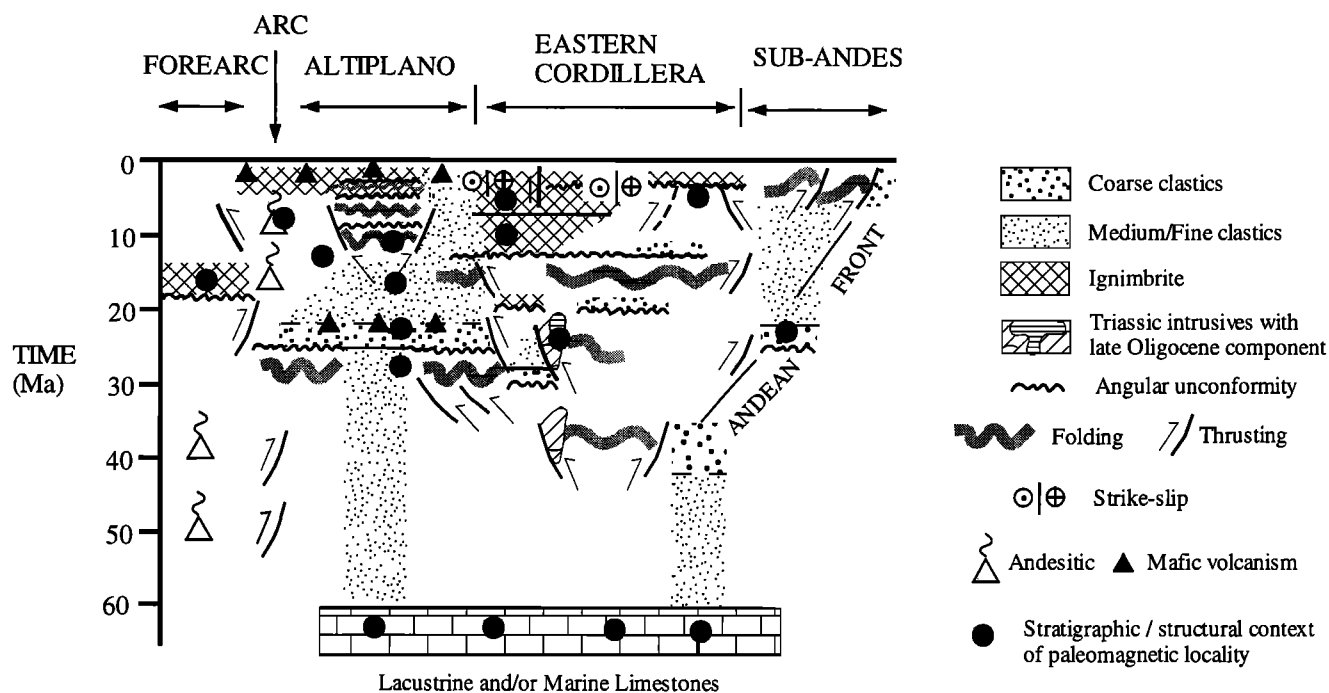


**Figure 3.** Diagram summarizing the distribution and timing of deformation and sedimentation in the central Andes for a generalized east-west transect between the latitudes 16°S and 22°S [after *Lamb et al.*, 1997]. Paleomagnetic localities in this and previous studies are shown in the context of this diagram.

The limestone specimens were generally weak, with initial magnetizations (natural remanent magnetizations (NRM)) in the range 0.1–3.6 mA m<sup>-1</sup>. A low unblocking temperature component, with variable magnetic intensities, was generally removed at temperatures between 0 and 200°C (Figure 9, specimens OTA-B2-4, CAN-D7-4, AD-D2-3, and COP-B1-3). At higher temperatures, stepwise thermal demagnetization progressively removed a second (Figures 9 and 10), or sometimes a third, component. The third component was identified in specimens from the Otavi and Camargo synclines (Figure 9, specimens OTA-B2-4 and CAN-D7-4). The magnetization intensity was generally reduced to ~50% of the NRM intensity at 400°C in pink limestone (specimens SAR, CHA, PAL, TUM, and CAZ, Figures 10 and 11). However, in gray limestones the intensity was <10% of the NRM at 400°C (Figure 9, specimens CAN-D7-4 and CAN-B4-4). The high unblocking temperature components in pink limestones were only completely removed above 600°C (Figure 10). IRM studies reveal a rapid increase in acquisition of induced magnetization up to about 300 mT, with either saturation (Figure 9b) or a slow further increase (Figures 9b and 10b). This behavior suggests that (ti)-magnetite ± hematite are the main magnetic carriers; the pink color is due to disseminated hematite.

The bulk of specimens showed a reversed polarity high unblocking temperature component during demagnetization. Some specimens showed two different reversed polarity components, isolated at moderate and high unblocking temperatures, as well as a normal low unblocking temperature component essentially parallel to the present-day field (Figure 9, C<sub>3</sub> component in specimen OTA-B2-4).

### 3.3. Oligo-Miocene Red Beds

Thick sequences of red sandstones and siltstones are exposed in the fold and thrust belt on the eastern margin of the Bolivian Andes, referred to as the sub-Andean zone (Figures 3, 6, and 8c).

The stratigraphically highest sequences are exposed in the cores of tight synclines along the length of the sub-Andes, and beds generally dip steeply, between 45° and vertical. Here, basal conglomerates referred to as the Petaca Formation, overly coarse white Cretaceous quartzites. Mammal fossils found in the Petaca Formation suggest an Oligo-Miocene age [Marshall and Sempere, 1991]. This age is supported by fission track dates of ~24 Ma [Jordan et al., 1997] for zircons in tuffs just above the Petaca sequence, outcropping close to Monteagudo (near localities MO 1-3). Above the basal conglomerates, there is a monotonous sequence of alternating coarse to medium parallel-bedded red sandstones units intercalated with dark brown-gray fine sandstones, siltstones and mudstones deposited in a fluvial environment. The main exposures are in the banks of rivers. However, because the rivers generally flow along the structural trend, only a limited stratigraphic thickness is exposed in any one place. In these sequences, individual localities consisted of 5 to 14 samples collected from a succession of siltstone or fine sandstone interbeds over a stratigraphic thickness of several meters to several tens of meters. Groups of three closely spaced localities, up to a few kilometers apart, were sampled at four points along the length of the western margin of the sub-Andean zone between 17.5°S and 23°S (Figure 6).

Initial intensities ranged between 20 and 0.5 mA m<sup>-1</sup>. During thermal demagnetization, a normal polarity low unblocking temperature component was often removed between 0 and 200°C, accompanied by a drop in intensity to ~50% of the NRM intensity. This component was generally subparallel to the present-day field. Above 200°C, many samples showed complex demagnetization behavior, often with pronounced excursions in which the specimen's magnetic intensity increased in strength then progressively decreased again, giving rise to a zig-zag type of Zijderveld plot. For example, no stable magnetizations were measured in specimens from SAL1. Demagnetization in these specimens was

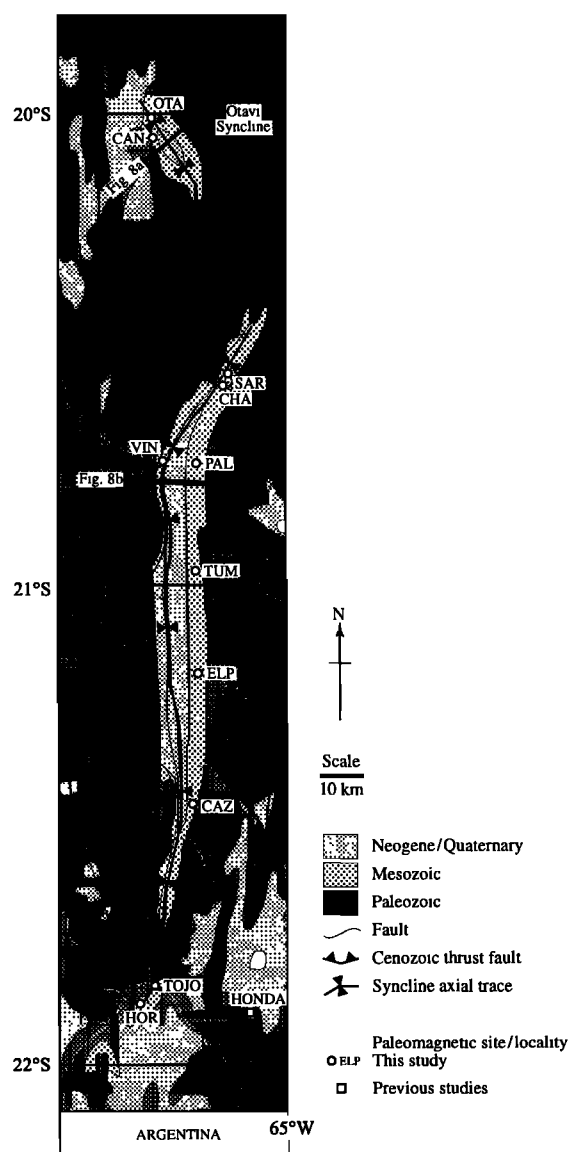


**Figure 4.** Detailed geological map (modified from *Bolivian Geological Survey (GEOBOL) and Yacimientos Petroliferos Fiscales Bolivianos (YPFB)* [1978]) of the Otavi and Camargo synclines in the southern part of the Bolivian Eastern Cordillera (see Figure 2 for location). These folds form asymmetrical and east verging sinuous folds, extending for several hundred kilometers along strike, defined by folded Upper Cretaceous-Eocene sedimentary sequences which rest unconformably on deformed Silurian and Ordovician flysch-like deposits. Bold lines mark the lines of cross sections illustrated in Figure 8a (Otavi syncline) and Figure 8b (Camargo syncline). Paleomagnetic localities in Upper Cretaceous-Paleocene pink and grey limestones are shown (see Table 1).

too erratic to define any stable magnetic components. However, in about half of the specimens analyzed, an overall trajectory could be observed, albeit often “noisy” (Figure 12, specimen MO3-C1-2), toward the origin, with a pronounced drop in intensity between about 500°C and 600°C. This trajectory defined both normal (Figure 12, specimen BE3-D3-1) and reversed polarity (Figure 12, specimens MO3-B3-2, IN1-B5-1, BE2-A3-1) magnetizations. A small amount of magnetization, constituting 10% of the total intensity, persisted to temperatures over 600°C. These results suggest that the main magnetic carrier in most samples is (ti)-magnetite, with subsidiary hematite (the hematite staining causes

the red-brown color). In some specimens the demagnetization essentially “stalled” at temperatures between 350°C to 550°C, though the direction of magnetization in the sample remained more-or-less constant (Figure 12, specimens IN1-A3-1 and BE1-B2-6). In these specimens, hematite seems to be the main carrier. These conclusions are supported by IRM measurements, which show a major acquisition of induced remanence below 300 mT, and a small amount of continued acquisition occurs up to 800 mT (Figure 12b).

### 3.4. Miocene Volcanic and Intrusive Rocks

Samples from a wide range of Miocene volcanic and plutonic rocks were collected in this study, including lavas, ignimbrites, and shallow to intermediate depth intrusions.

1. A subhorizontal lava flow(s) was sampled in an area of ~10 km<sup>2</sup> on the eastern flank of the deeply eroded 8-9 Ma Cerro Tres Monos volcano [Baker and Francis, 1978]. This volcano lies in northern Chile near Yuma, north of Volcan Ollague and close to the border with Bolivia (Figure 2, (sites O11-3)). It was not possible to determine whether one or more flows were sampled; for this reason, the sampling region was treated as a single site.

2. Four separate rhyolitic ignimbrites (Tahua Formation), dipping up to 30° and dated at ~14 Ma (Ar-Ar age on biotite (E. Soria-Escalante, personal communication, 1994)), were sampled on the northern and southern margins of the Salar de Uyuni in the central part of the Altiplano (Figure 7, sites TAH1-3 and YON).

3. A laterally extensive sequence of mafic lavas and shallow level basaltic and pyroxenite sills, dated at 22-24 Ma (Figures 7 and 8d [Kennan *et al.* 1995; Lamb and Hoke 1997]), outcrops in the central and northern parts of the Altiplano, extending along strike for over a 100 km. A single basaltic sill was sampled near Tambo Tambillo (Figure 7, site Chiar). The sill, together with the enclosing stratigraphy, dips at ~50° on the western limb of a regional NW trending syncline [Kennan *et al.*, 1995; Lamb and Hoke, 1997].

4. Four ignimbrites were sampled in a laterally extensive sequence, several hundred meters thick, of rhyolitic ignimbrites and ash fall deposits, outcropping on the western margin of the Eastern Cordillera and referred to as the Los Frailes Formation (Figures 3 and 7, sites JAP, HUA, TR, and POR). Los Frailes ignimbrites range in age from ~12 Ma at the base to ~6 Ma [Kennan *et al.*, 1995]. They are essentially undeformed, except for some local faulting, and mantle an older subhorizontal land surface with subdued relief at an altitude of ~4000 m.

5. A medium-grained dioritic (hornblende-bearing) shallow intrusion with abundant mafic xenoliths was sampled near the township of Comanche in the northern Altiplano, outcropping in an area slightly less than a square kilometer (site COM in Figure 2). This body intrudes middle Miocene red bed sequences and has been dated at ~14 Ma [Lavenue *et al.*, 1989]. The enclosing sediments are folded, dipping at ~25°. This folding postdates the emplacement of the intrusion, affecting sedimentary sequences as young as ~9 Ma [Lamb and Hoke, 1997].

6. Samples were taken from a coarse-grained granodioritic intrusion (Mina Cunurana intrusion), which outcrops in an area of several square kilometers, SE of Potosi at the southern end of the Kar-Kari extrusive/intrusive complex (Figure 7, site MC). Biotites from the granodiorite have been dated, using the K-Ar method, at ~24 Ma [Evernden *et al.*, 1977; Grant *et al.*, 1979], and it intrudes Paleozoic shales and sandstones. The intrusion lies on the northern limb of an approximately east trending syncline in the country rock and may have been tilted ~25° to the south (S. H. Lamb, unpublished field data, 1991).

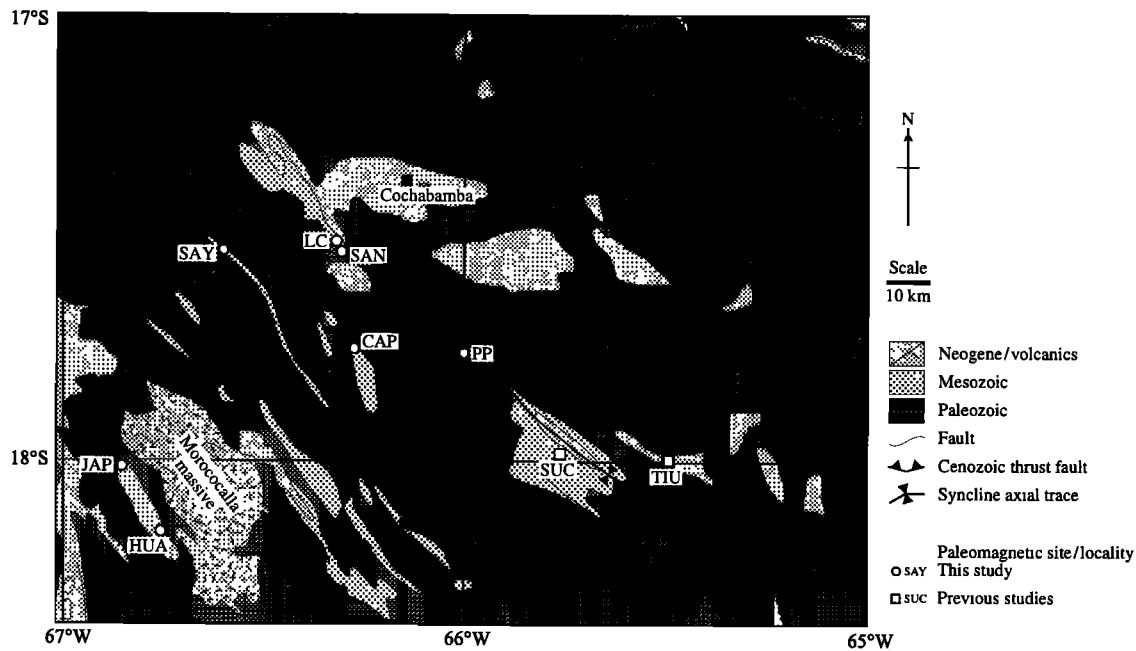


**Figure 5.** Geological map (modified from *Bolivian Geological Survey (GEOBOL) and Yacimientos Petroliferos Fiscales Bolivianos (YPFB)* [1978]) of the Eastern Cordillera in the vicinity of Cochabamba (see Figure 2 for location), showing prominent synclines of Upper Cretaceous sequences and also Plio-Miocene extensional basins bounded by WNW trending sinistral normal faults which have been active since the early Miocene [Kennan, 1994]. Paleomagnetic localities in Upper Cretaceous-Paleocene pink oolitic and micritic limestones, and upper Miocene ignimbrites (Morococalla massive) are also shown (see Table 1 and 3). Declination anomalies, determined for localities in the central part of this region, define domain 3b.

**3.4.1. Demagnetization of volcanic rocks.** Initial magnetization intensities (NRM) of volcanic specimens were usually several orders of magnitude greater than those for sedimentary samples, ranging between 4 and 2080 mA m<sup>-1</sup>. Andesitic lavas had particularly high intensities (Figure 13, specimen OL2-II-2); rhyolitic ignimbrites were generally much weaker (Figure 13, specimen YON-A1-3), but could also have high intensities (Figure 13, specimen HUA-B7-4). Some of the highest-intensity specimens came from rock faces low down within a narrow and deep railway cutting and are unlikely to be the effect of lightning strikes, but more likely they reflect the high magnetite content of the lavas. Thermal demagnetization showed that the magnetization had unblocked by >95% at 580°C, suggesting that (ti)-magnetite is the principal magnetic carrier. IRM acquisition studies show that saturation of induced magnetization is reached by 300 mT, again suggesting (ti)-magnetite as the magnetic carrier (Figure 13b). The ignimbrites from the Los Frailes satellite massif and Altiplano generally displayed simple demagnetization responses, with a weak secondary component unblocked by 100°C. A strong and well-grouped high unblocking temperature component could be readily identified in most, suggesting that these ignimbrites were emplaced hot (>200°C) and acquired a magnetization on cooling (Figure 13, specimen HUA-B7-4). However, some of the other volcanic specimens showed overlapping unblocking temperature characteristics, with a pronounced curved trajectory on a Zijderveld diagram. This was particularly clear in coarse and poorly welded ignimbrites in the Tahua formation (Figure 7, locality TAH). Great circle analysis of this type of unblocking behavior was used to determine a mean primary magnetization (Figure 13d), though distinct low and high unblocking temperature components could be identified in specimens from one Tahua Formation ignimbrite (Table 3, site TAH1).

**3.4.2. Demagnetization of intrusive rocks.** Coarse- to medium-grained granodioritic (Figure 7, locality MC) and dioritic (Figure 2, locality COM) intrusions, outcropping in both the Altiplano and Eastern Cordillera, yield clear high unblocking temperature components of magnetization after thermal demagnetization. Specimens from locality MC showed a reversed polarity high unblocking temperature component, compared to normal polarity for the lower unblocking temperature component (Figure 13, specimen MC-C2-2). Specimens from locality COM consisted of both the main body of the dioritic intrusion and also mafic xenoliths. A consistent high unblocking temperature component was isolated from mafic xenolith specimens (Figure 13, specimens COM-A3-4 and COM-G3-3). Specimens from the main body of the intrusion generally failed to reach a stable point during thermal or alternating field demagnetization, but the direction of magnetization followed well-defined great circle trajectories; great circle analysis was used to define a mean primary magnetization (Figure 13).

## 4. Data Analysis

### 4.1. Statistical Analysis and Grouping of Data

The use of paleomagnetic data for tectonic analysis depends crucially on (1) determining the age of the magnetization and (2) ensuring that it is possible to group data so that paleosecular variation is averaged. It is important to distinguish between primary magnetization, acquired close to the time of formation of the rock, and a secondary magnetization acquired at some later date and related to a subsequent phase of diagenesis or low-grade metamorphism, or surface weathering.

Sedimentary rocks sampled in this study are mainly fine-grained interbeds in alluvial sequences or micritic and bioclastic

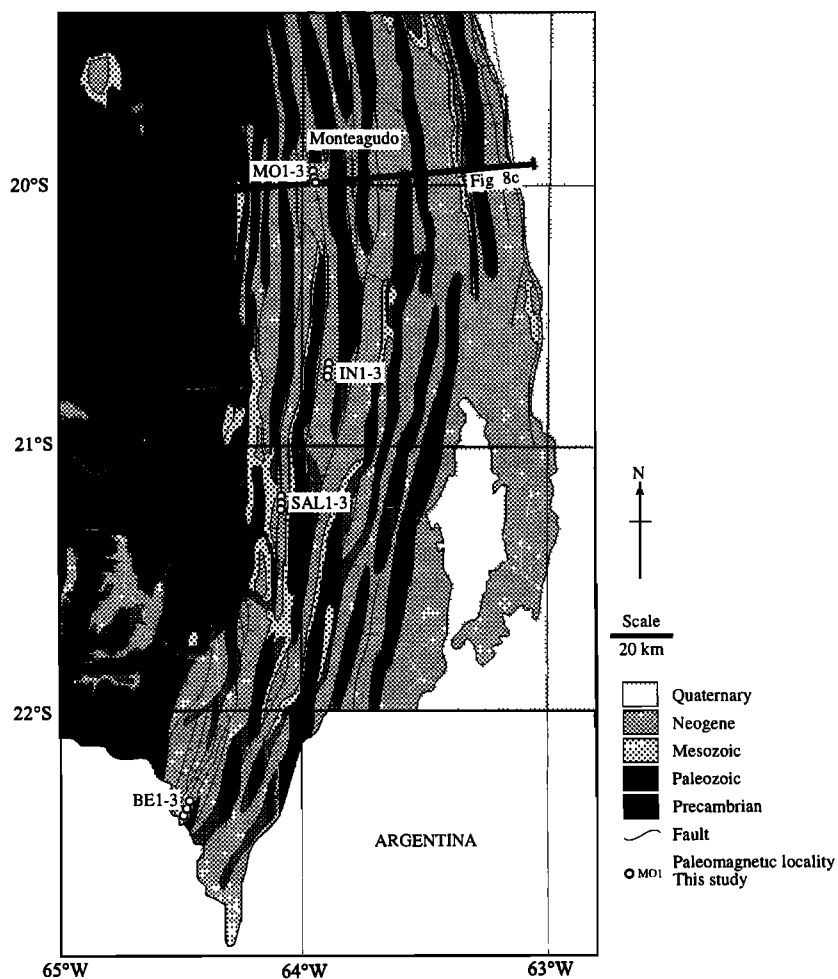


**Figure 6.** Geological map (modified from *Bolivian Geological Survey (GEOBOL) and Yacimientos Petroliferos Fiscales Bolivianos (YPFB)* [1978]) of the sub-Andean zone, south of the bend in the Bolivian orocline (see Figure 2 for location). This region has a pronounced structural trend, defined by tightly folded and faulted synclines and anticlines which swing round from a roughly N-S trend in the north to more NE-SW farther south. Synclinal cores consist of sequences, several kilometers thick, of Oligo-Miocene and Pliocene red beds. Paleomagnetic localities in Oligo-Miocene red beds (see Table 2), as well as the line of the cross section, illustrated in Figure 8c, are also shown.

limestones; in both cases there is evidence for bioturbation prior to lithification. Any well-grouped magnetization was clearly acquired during or after diagenesis, most likely over a protracted period. For this reason, the magnetizations defined from individual specimens, sampling individual small-scale domains of bioturbation, diagenesis, or even sedimentation, are as likely as those from different samples (cores) to record a range of epochs of the Earth's magnetic field (see sections 4.2 and 4.3). In most cases, only one specimen was obtained from a single sample (core), and in all cases, specimen groupings are identical, within error, to sample groupings. In Tables 1 and 2, the number of specimens and the number of samples are given for each locality, as well as the stratigraphic thickness spanned by sampling. Locality means are based on groupings of specimen magnetic components (Figure 14). Magnetizations measured in individual specimens from volcanic rocks or coarse-grained intrusions were grouped to produce a site mean (Table 3).

#### 4.2. Fold Tests and the Timing of Magnetization

If the rocks were deformed since the magnetization was acquired, then the magnetization must be corrected for this deforma-

tion to determine its original direction. In this study, a simple tectonic tilt correction was applied by rotating the site mean vector about the strike of the bedding, so that the layering is restored to the horizontal.

The tilt correction allowed a discrimination between predeformation and postdeformation components of magnetization. In samples that contained two components of magnetization, revealed by stepwise demagnetization, the lower unblocking temperature component of the two usually had a direction which was more-or-less parallel to the recent geocentric axial dipole field direction, with either a reversed or normal polarity; the higher unblocking temperature component often had a direction that was distinct from this. After correction for the stratal tilt this magnetization typically had an inclination similar to that expected for rocks of the same age and location, in a South American reference frame (see discussion on reference paleomagnetic poles below). For localities, or groups of localities, where stratal orientation varied significantly, i.e., on different limbs of a fold, the clustering of data prior to tilt correction was compared to that afterward, comprising a modified McElhinny Fold Test [McElhinny, 1964; McFadden and Jones, 1981]. This test was carried out for several

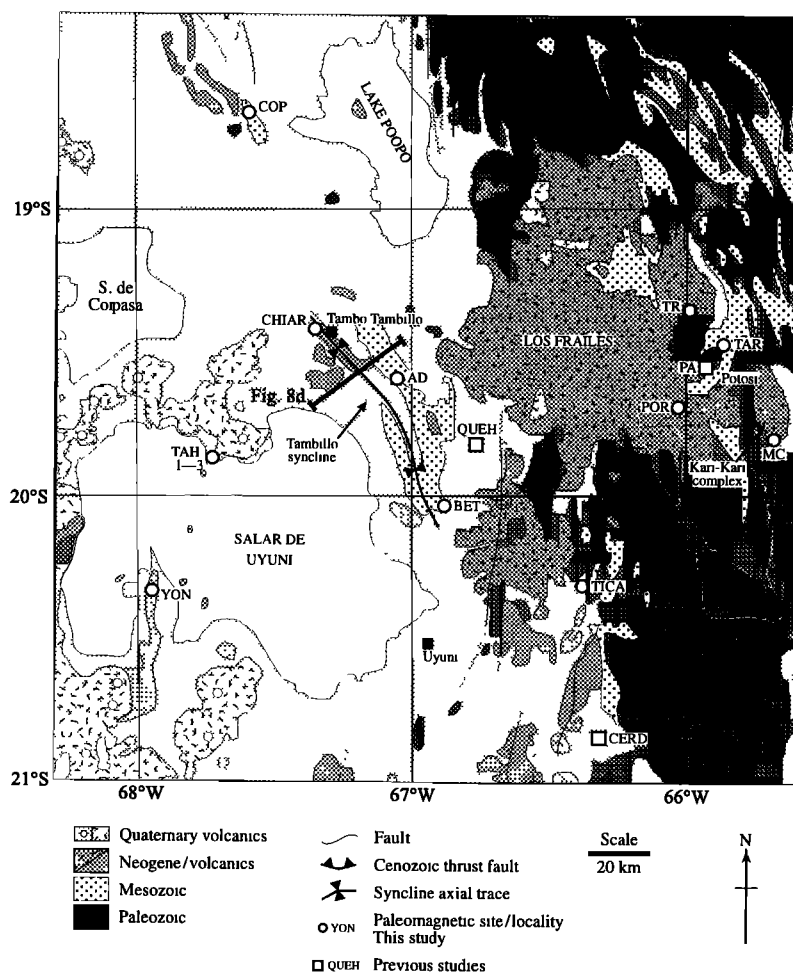


**Figure 7.** Geological map (modified from *Bolivian Geological Survey (GEOBOL) and Yacimientos Petroliferos Fiscales Bolivianos (YPFB)* [1978]) of the western margin of the Eastern Cordillera and the central Altiplano (see Figure 2 for location). The eastern part of this region consists of deformed Paleozoic flysch deposits, with infolded Cretaceous sequences, which are capped by extensive regional ignimbrites of middle to upper Miocene age, culminating in the 6-8 Ma Los Frailes ignimbrites. An elongate lower Miocene extrusive/intrusive ignimbrite (Kari-Kari) complex, intruded by a granodiorite body at its southern end (Mina Cunurana intrusion), outcrops immediately southeast of Potosi. Plio-Pleistocene salars form extensive regions in the Altiplano (Salar de Uyuni and Coipasa), and Lake Poopo is a very shallow body of water farther north. On the eastern margin the region is mainly andesitic volcanic rocks of the active and Miocene volcanic arc. The northeast corner of the Salar de Uyuni is underlain by tightly folded Upper Cretaceous-Paleogene sequences and Miocene red beds and volcanics. Bold line shows the line of the cross section, illustrated in Figure 8d. Paleomagnetic sites or localities are also shown (see Tables 1 and 3).

groups of localities in Upper Cretaceous - Paleocene limestones from the Cochabamba area, the Otavi syncline (localities CAN and OTA), and northern part of the Camargo syncline, and groups of localities in folded fine sandstones and siltstones in the sub-Andean zone. For these localities or groupings of localities the fold test was passed at the 99% confidence level (Table 5). Finally, the presence of stratigraphically-separated specimens with either normal or reversed polarity magnetizations and antipodal orientations was used as supporting evidence that the magnetization is primary.

Sometimes, specimens contained two high unblocking temperature components of magnetization, as well as a low unblocking temperature component parallel to the present-day field. The best examples came from rocks of the Otavi syncline (Figure 9a, localities OTA, CAN), where two well-defined high unblocking

temperature components, which were only unblocked at temperatures above 300°C, had reversed polarities. The lower unblocking temperature component of these had an inclination similar to that of the present-day local magnetic field, without a tilt correction, while the higher unblocking temperature component only had the expected inclination after the tilt correction was applied. This strongly suggests that the limestones acquired both a primary magnetization prior to tilting and a "hard" secondary component after tilting.

Distinguishing between primary and secondary magnetizations was difficult for several localities in Upper Cretaceous-Paleocene limestones in the Camargo syncline (Table 1 and Figures 8b and 10a, localities PAL, TUM, ELP, and CAZ), where dips were <20°. These localities are in oolitic or micritic limestone with a red or pink hematitic matrix and show a well-defined magnetiza-

Table 1. Paleomagnetic Data for Upper Cretaceous to Palaeocene Limestones Analyzed in This Study

Locality or Site <sup>a</sup>	Label	Lat°S/Long°W	Age, Ma	Lithology /Stratigraphy <sup>b</sup>	N <sup>c</sup>	D <sup>d</sup>	I <sup>e</sup>	$\alpha_{95}$ <sup>f</sup>	k <sup>g</sup>	$\sigma^d$	Bedding	Corr. D <sup>h</sup>	Corr. I <sup>e</sup>	RZAR <sup>i</sup>	FZAF <sup>j</sup>	
Andamarca	COP	18.69/67.61	65±5	B/20 m	9/5	173	38	7	63	13	307/33N	141 <sup>f</sup>	56 <sup>f</sup>	-31±11	13±7	
	AD	19.59/67.08	80±5	B+M/60 m	8/7	176	2	5	120	9	307/66N	150 <sup>f</sup>	44 <sup>f</sup>	-19±6	4±5	
	BET	20.04/66.90	65±5	M/5 m	9/6	141	39	5	114	9	152/50W	179 <sup>f</sup>	31 <sup>f</sup>	7±6	-14±5	
	TICA	20.27/66.34	65±5	M/70 m	14/13	138	19	12(12)	12(12)	28	~176/40-80W	178 <sup>f</sup>	47 <sup>f</sup>	6±14	2±10	
La Cabana <sup>a</sup> Santibanez Sayari Capinota <sup>a</sup> PP Tarapaya <sup>a</sup> Otavi (C <sub>p</sub> ) <sup>a</sup> Otavi (C <sub>s</sub> ) <sup>a</sup> Cancha (C <sub>p</sub> ) Cancha (C <sub>s</sub> ) Cancha (C <sub>p</sub> ) Chañar Mayu A+B <sup>a</sup> Garcaca <sup>a</sup> Vina Grande (C <sub>p</sub> ) Vina Grande (C <sub>s</sub> ) Balcon <sup>a</sup> Tunusla <sup>a</sup> El Puente Carrizal <sup>a</sup> Tojo Homos	LC	17.50/66.33	65±5	M/2 m	9/5	224	5	6	72	11	343/40E	215 <sup>f</sup>	39 <sup>f</sup>	(43±7)	(-2±6)	
	SAN	17.52/66.30	65±5	M/6 m	9/9	211	0	5	120	9	332/61E	191 <sup>f</sup>	48 <sup>f</sup>	19±7	7±5	
	SAY	17.62/66.53	65±5	M/14 m	9/8	110	55	5	10	10	156/50W	195 <sup>f</sup>	56 <sup>f</sup>	2±8	14±5	
	CAP	17.77/66.29	65±5	B+M/2 m	5/3	033	-18	21	58	29	326/31E	030 <sup>f</sup>	-46 <sup>f</sup>	(38±25)	(4±17)	
	PP	17.88/65.90	65±5	M/5.5 m	5/5	337	-46	10	180	13	150/20W	354	-39	2±11	-3±9	
	TAR	19.47/65.83	80±5	M/1.5 m	8/4	044	-17	5	74	12	010/80E	355 <sup>f</sup>	-35 <sup>f</sup>	(6±6)	(-5±4)	
	OTA	20.00/65.30	80±5	M+B/4 m	5/3	086	-75	9	79	12	048/55S	336 <sup>f</sup>	-43 <sup>f</sup>	(-14±10)	(2±8)	
	OTA	20.00/65.30	80±5	M+B/50 m	6/3	181 <sup>f</sup>	36 <sup>f</sup>	8	386	5	048/55E	002 <sup>f</sup>	-8	13±5	9±4	
	CANI	20.04/65.32	80±5	M+B/30 m	7/4	029	7	3	25	20	166/102W	172 <sup>f</sup>	49 <sup>f</sup>	3±13	8±9	
	CANZ	20.04/65.32	80±5	B+M/6 m	10/5	117	-5	10	37	16	334/77E	120	20			
	CAN	20.04/65.32	80±5	B+M/30 m	11/7	170 <sup>f</sup>	36 <sup>f</sup>	8	5(32)	45(16)		177 <sup>f</sup>	51 <sup>f</sup>	(5±11)	(5±7)	
	Chañar Mayu A+B <sup>a</sup>		20.62/65.19	65±5	M/0.8 m	10/10	199	36	24(8)	11(39)		188 <sup>f</sup>	51 <sup>f</sup>	(16±15)	(5±10)	
	CHA		20.62/65.19	65±5	M/2 m	6/6	163	28	22(11)	17		201 <sup>f</sup>	43 <sup>f</sup>	29±15	-3±11	
	SAR		20.73/65.28	65±5	M/11 m	9/5	259	18	13	82	10	033/78E	348	11		
	VIN		20.73/65.28	65±5	M/11 m	10/7	008 <sup>f</sup>	-40 <sup>f</sup>	5	82	10	033/78E	348	11		
	VIN		20.73/65.28	65±5	B/1 m	13/5	175	47	3	155	7	218/13W	189	55	(17±6)	(9±4)
BALCON <sup>a</sup>		20.73/65.19	65±5	B/1 m	13/5	175	47	3	155	7	218/13W	189	55	(17±6)	(9±4)	
TUNUSLA <sup>a</sup>		20.97/65.21	65±5	B/4 m	5/4	183	41	11	46	15	192/15W	196	42	(24±12)	(-4±10)	
EL PUENTE		21.27/65.18	65±5	B+M/7 m	14/11	358	-44	10	18	22	161/20W	014	-36	22±11	-10±9	
CARRIZAL <sup>a</sup>		21.44/65.22	65±5	B+M/3 m	7/6	186	40	9	22	14	181/20W	201	36	(29±10)	(-11±8)	
TOJO		21.82/65.32	65±5	B+M/5 m	4/4	181	43	24	16	29	188/27W	206	40	34±26	-7±20	
HOMOS		21.86/65.34	65±5	B+M/24 m	12/12	258	38	10	20	21	048/47E	214 <sup>f</sup>	45 <sup>f</sup>	42±12	-2±9	

<sup>a</sup> C<sub>p</sub> and C<sub>s</sub> refer to high unblocking temperature (primary) and low unblocking temperature (secondary) components.  
<sup>b</sup> Lithology (B, bioclastic limestone; M, micritic limestone or calcareous shale, S, stromatolite), sampled stratigraphic thickness in meters.  
<sup>c</sup> Number of specimens/samples (see text).  
<sup>d</sup> D, declination, I, inclination,  $\alpha_{95}$ , 95% angular confidence limit; k, Fisher precision parameter;  $\sigma$ , angular dispersion; Corr. D and Corr. I are tilt corrected. Values in parentheses refer to tilt-corrected data.  
<sup>e</sup> RZAR, vertical axis rotation and standard error; FZAF, flattening and standard error; calculated with respect to Roperch and Carlier's [1992] 60 and 80 Ma South American reference palaeomagnetic poles, using the method of Butler [1992]. Values in parentheses are for localities with a stratigraphic thickness < 5 m.  
<sup>f</sup> Magnetizations constrained by tilt or fold tests to have occurred either before or after tectonic tilting, the timings of other magnetisations are uncertain.  
<sup>g</sup> Localities have stratigraphic thicknesses < 5 m, and paleosecular variation may not be averaged (see text).

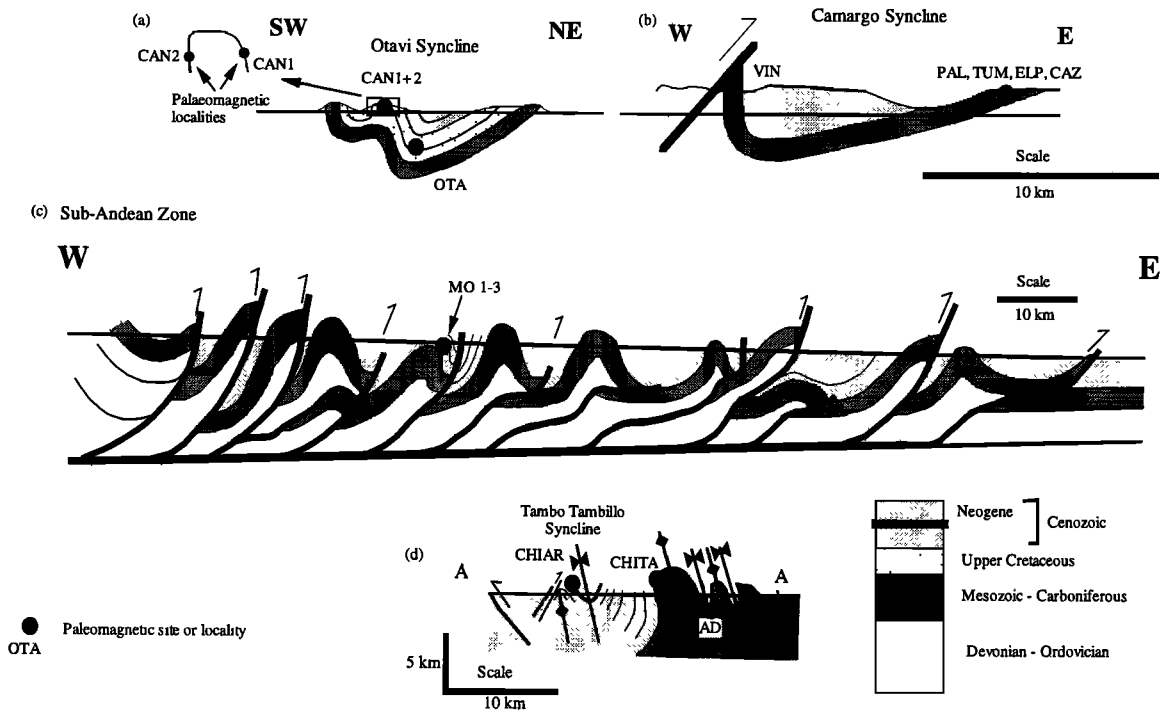


**Figure 8.** Geological cross sections through parts of the Bolivian Andes (see Figures 4, 6, and 7 for location), showing structural position, projected on to cross-section, of paleomagnetic localities. Cross sections are based on an interpretation of Landsat satellite images, combined with field measurements (S. Lamb, unpublished field data 1990-1998), data from published 1:100,000 and 1:1,000,000 geological maps [*Bolivian Geological Survey (GEOBOL)*, 1962-1992; *Bolivian Geological Survey (GEOBOL)* and *Yacimientos Petroliferos Fiscales Bolivianos (YPFB)*, 1978], and seismic reflection profiles (with kind permission of Yacimientos Petroliferos Fiscales Bolivianos (YPFB)). (a) NW trending, east-verging and doubly-plunging (canoe-shaped) synclinal and anticlinal Otavi structure (see Figure 4 for location). (b) Central part of the regional NW to north trending Camargo syncline (see Figure 4 for location). The steep dip of the western limb made it possible to distinguish pretilt and posttilt magnetizations. However, the age of magnetization on the gentle limb is unclear (see text). (c) Sub-Andean zone on the eastern margin of the Bolivian Andes (see Figure 6 for location). The structure is an east verging fold and thrust belt above a west dipping sole thrust. Paleomagnetic localities are in Oligo-Miocene red beds in the cores of tight synclines. (d) Tightly folded (Tambillo syncline) Upper Cretaceous to Miocene sequences in the Altiplano, near Tambo Tambillo (see Figure 7 for location). The structural trend is sinuous, varying from N-S to NW-SE.

tion, unblocked at temperatures up to 650°C; tilting of the beds is too small to be used to test the age of magnetization. IRM studies suggest that generally (but not always), when the magnetization passes the fold test, the magnetic carrier is likely to be (ti)magnetite and shows saturation above 300 mT. However, in many cases, specimens that display more linear IRM plots contain a “hard” secondary component that fails the fold test (Figures 9b and 10b). For instance, the high unblocking temperature magnetic component in limestone specimens from a steeply dipping part of the Camargo syncline (specimens VIN-C5-1 and VIN-F2-3, Figures 4, 8b, and 10) fails the tilt test. IRM plots for these specimens are distinctly linear (Figure 10b), without the marked increase in acquisition below 300 mT. IRM plots for localities PAL, TUM, and CAZ show similarities to this (Figure 10b and compared with Figure 9b). One possibility is that the magnetization of these specimens was strongly overprinted in the upper Miocene–Pliocene. At this time, substantial parts of the Eastern Cordillera had a low relief as a result of regional peneplanation in low gradient drainage systems [Gubbels *et al.*, 1993; Kennan *et al.*, 1997; Lamb *et al.*, 1997]. The limestones would have been within 2 km of the surface, presumably within a regional aquifer system. These conditions could have allowed the limestones to de-

velop a secondary porosity and cement that may have been associated with the acquisition of a “hard” secondary magnetization.

The analysis of magnetizations determined in this study (Tables 1 - 3) takes account of the criteria discussed above. Magnetizations which pass a fold or simple tilt test (see Table 5) or reversal test are assumed to be primary and are indicated. Those at other localities cannot be unambiguously dated.

#### 4.3. Paleosecular Variation

An issue in the interpretation of the mean magnetization for a particular locality is whether it records a geocentric axial dipole field or is biased by the effects of paleosecular variation. Studies of the Earth’s magnetic field during the Holocene suggest that the average position of the north geomagnetic field, averaged over periods as short as a few thousand years, coincides, within error, with the north geographic pole [Butler, 1992]. Paleomagnetic sampling in rocks from an individual locality spanning much more than  $10^4$  years of magnetization may be necessary to fully average the effects of paleosecular variation [Butler, 1992].

**4.3.1. Sedimentary sequences.** The long-term sedimentation rate for Oligo-Miocene fluvial red bed sequences in the Bolivian

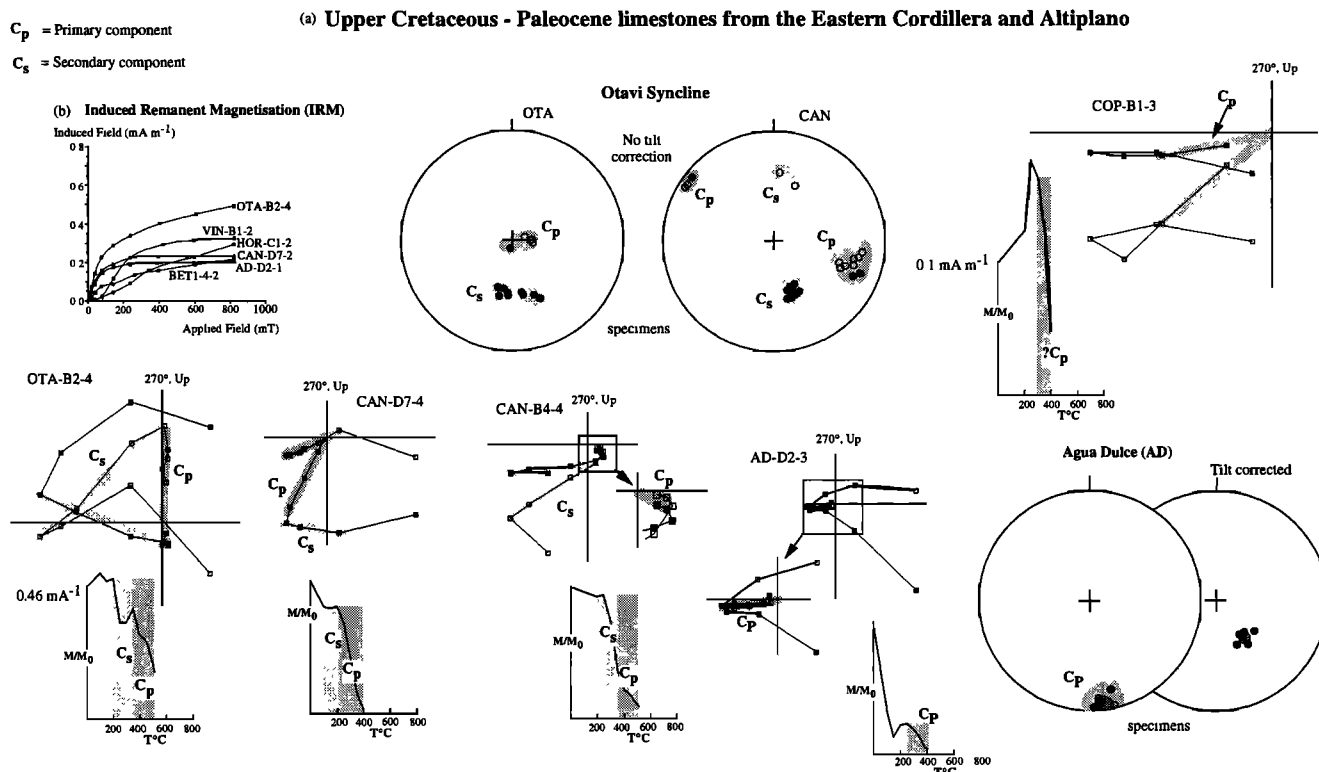


**Figure 9.** Demagnetization data (Zijderveld plots, total magnetization intensity plots, and equal-area stereonets) for Upper Cretaceous-Paleocene limestones from the Otavi syncline and elsewhere in the Eastern Cordillera and Altiplano (see Figures 2, 6, and 8). Solid dots on stereonets denote positive inclinations; open circles show negative inclinations. Zijderveld plots for representative samples, along with plots of magnetization intensities at each temperature step, are used to define unblocking trajectories: solid squares denote horizontal projection; open squares denote vertical projection. (a) The unblocking behavior defines magnetic components: (1) up to three low unblocking temperature normal and reversed polarity components (labeled  $C_s$  and with a light gray overlay), and (2) a higher unblocking temperature normal and reversed polarity component (labeled  $C_p$  and shaded). The highest unblocking temperature component ( $C_p$ ) has a direction before tilt correction which is significantly different from the present-day field (see text and Table 1); lower unblocking temperature components are more-or-less parallel to the Earth's present-day magnetic field, though with either normal or reversed polarities. The magnetization is almost completely unblocked above 500°C, suggesting (ti)-magnetite is the main magnetic carrier. (b) IRM studies also suggesting (ti)-magnetite as the carrier of the primary component. Samples which have passed a tilt test generally show rapid acquisition for an applied field up to ~300 mT, with little subsequent acquisition. However, specimens OTA-B2-4, HOR-C1-2, and BET1-4-2 (see Figure 10) have continued acquisition above 300 mT, suggesting the presence of hematite as a carrier.

sub-Andes is in the range 0.2-0.5 mm/yr [Jordan *et al.*, 1997]. These rates reflect both periods of rapid deposition and long periods of nondeposition or even erosion. Paleomagnetic sampling in this study was confined to the fine-grained flood plain or distal sheet flood interbeds, where most of the "time" in a sequence most likely lies. Measurements on Holocene and Neogene fluvial sequences [Leeder, 1975; Sadler, 1981; Friend *et al.*, 1989] suggest that flood plain muds, silts, and fine sandstones typically accumulate at a short-term rate of 0.5-1 m per thousand years in individual episodes during major floods [Friend *et al.*, 1989]. Beer [1990] estimates that a ~10 m sequence of fluvial sheet flood units, deposited in the Bermejo basin of northern Argentina around ~7.8 Ma, in a similar tectonic setting to the Bolivian Miocene red beds, contains a virtually continuous record over ~15,000 years. The much lower long term sedimentation rate (0.01-0.1 mm/yr) for the Bolivian Upper Cretaceous to Paleocene marine/lacustrine sequences [Sempere *et al.*, 1997] suggests that a similar thickness of micritic limestone and shale could represent a substantially longer period of deposition.

Normal and reverse polarity magnetizations were captured during paleomagnetic sampling of the Oligo-Miocene sub-Andean red beds (locality IN3) within a ~50 m stratigraphic section. The chances of finding both polarities in this section would be extremely small if the section represented  $<10^4$  years but much more likely if sampling spanned hundreds of thousands of years, as suggested by the long-term sedimentation rate. At Los Hornos and Vina, within Upper Cretaceous to Paleocene limestones in southern Bolivia (Table 1 and Figure 10, localities HOR and VIN), normal polarity magnetizations were found within 5-7 m thick intervals of the sections, bounded above and below by reverse polarity magnetizations. The magnetostratigraphy for this period suggests that these excursions are on a timescale of at least several tens of thousands of years [Sempere *et al.*, 1997].

The previous discussion suggests that a stratigraphic thickness greater than ~10 m of Oligo-Miocene red beds in the sub-Andes represents several tens of thousands of years of deposition. A comparable time span may be represented by as little as ~5 m of Upper Cretaceous to Paleocene limestones and shales in the East-

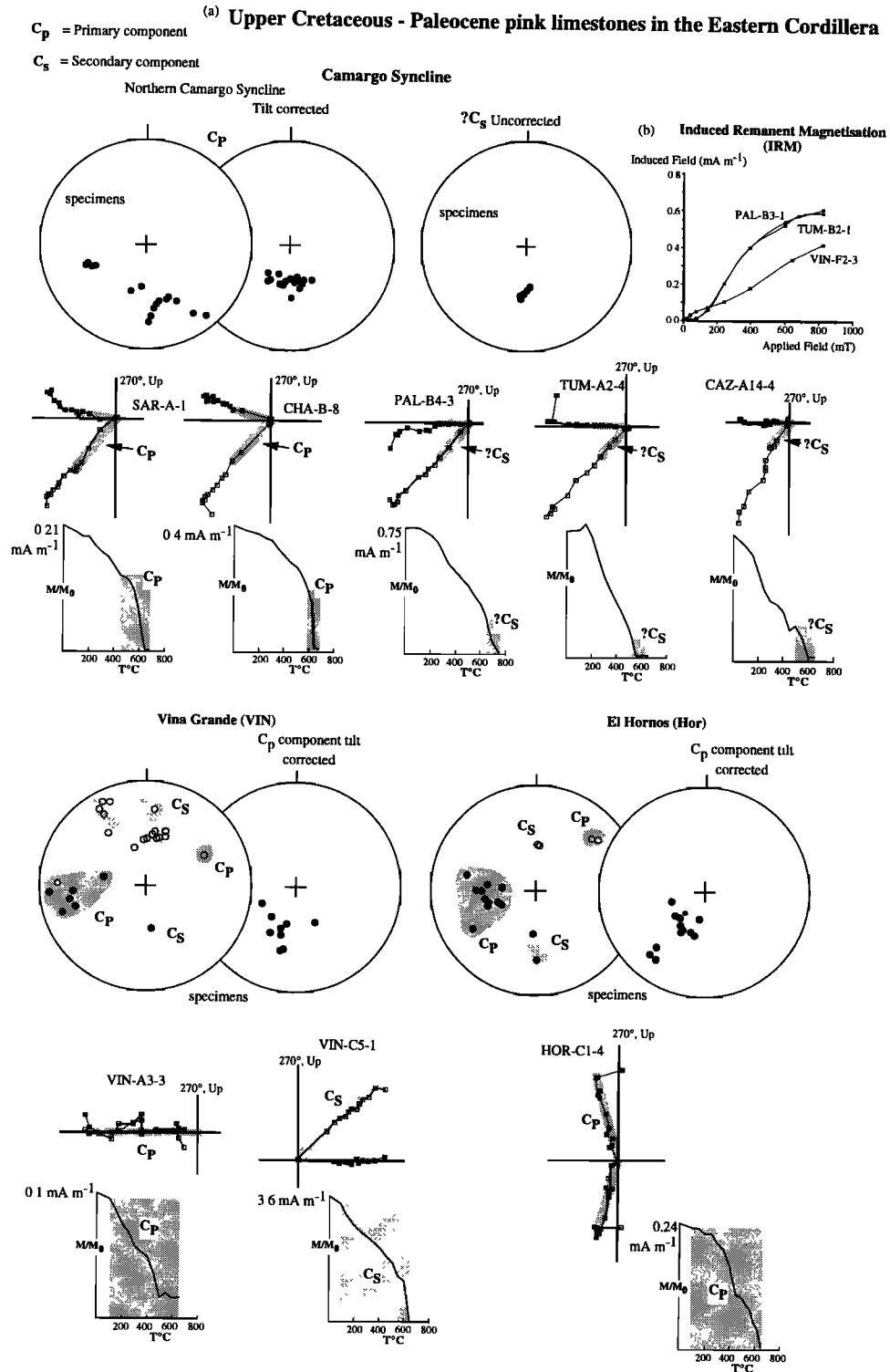


**Figure 10.** Demagnetization data (Zijderveld plots, total magnetization intensity plots, equal-area stereonets) for Upper Cretaceous-Paleocene pink micritic and oolitic limestones from the Camargo syncline (see Figures 2, 4, and 8 and caption for Figure 9). Solid circles on stereonets denote positive inclinations; open circles denote negative inclinations. (a) Magnetization is not completely unblocked until temperatures above 650°C, suggesting some hematite along with (ti)-magnetite as the magnetic carriers. Sample VIN-C5-1 shows a uniform magnetization component during thermal demagnetization, which persists to temperatures over 600°C. However, this component has a direction more-or-less parallel to the Earth's present-day field when uncorrected, but with an unrealistic inclination after tilt correction. This "hard" component is therefore interpreted as secondary ( $C_s$ ), acquired after folding. This result begs the question whether 'hard' components in other specimens from the Camargo syncline (e.g., PAL, TUM, CAZ) are also secondary; the shallow dips of the strata preclude a tilt test. (b) Magnetization trend in IRM studies for selected specimens; specimens with a more linear trend, such as VIN-F2-3, failed a fold test (Figure 9b).

## COCHABAMBA (Domain 3b)

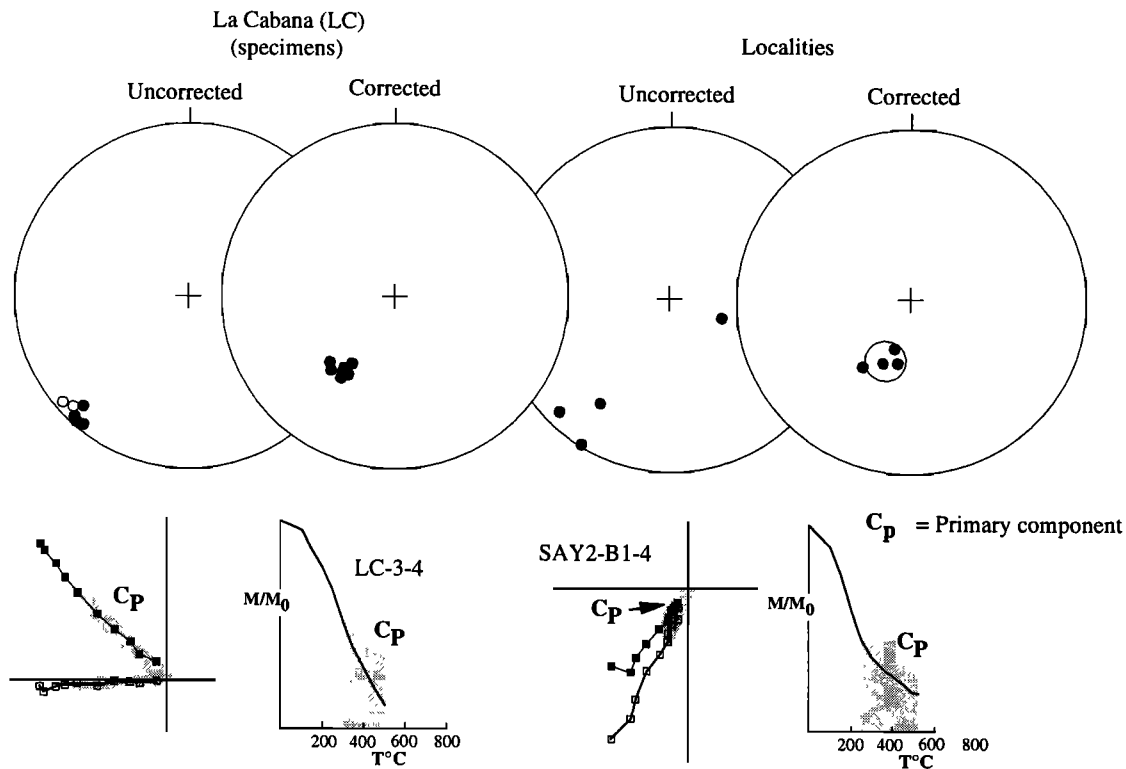


**Figure 11.** Demagnetization data (Zijderveld plots, total magnetization intensity plots, equal-area stereonets) for Upper Cretaceous-Paleocene pink micritic and oolitic limestones from the Cochabamba area (see Figures 2, 5 and caption to Figure 9). Solid circles on stereonets denote positive inclinations; open circles denote negative inclinations. Thermal demagnetization defines a clear reversed polarity component (labelled  $C_p$  and shaded), unblocked between  $\sim 300^\circ\text{C}$  and  $550^\circ\text{C}$ . The stereonet plots show that this magnetization is well grouped within a single locality (LC) and between localities after the tilt correction (see Table 1), with an inclination which is the same as that expected for this location and age. The tilt-corrected magnetization has a clockwise declination anomaly  $\sim 30^\circ$ , suggesting clockwise rotation about a vertical axis of these sites since the magnetization was acquired; these define domain 3b (see Figure 15).

ern Cordillera and Altiplano. Paleomagnetic sampling of these sequences is likely to be capable of averaging paleosecular variation. However, because of the high failure rate in obtaining well-defined magnetic components during thermal demagnetization, a few localities span  $<10$  meters of red beds or 5 m of limestones (localities indicated in Tables 1 and 2). It is plausible, but not certain, that the grouped magnetizations within these localities also average paleosecular variation. This uncertainty can be considerably reduced by grouping the mean magnetizations for a number of closely spaced localities (Table 4), comprising altogether several tens to hundreds of meters of stratigraphic thickness.

**4.3.2. Volcanic and intrusive rocks.** Individual ignimbrite units in the central Andes often have a remarkably consistent magnetization between widely separated sites, even though the inclination is significantly biased away from that expected for a geocentric axial dipole field [Somoza *et al.*, 1996, 1999; Roperch *et al.*, 2000]. The most plausible explanation is that the acquisition of magnetization occurred on geologically short timescales during individual volcanic eruptions and is strongly influenced by paleosecular variation. It was difficult to devise a sampling strategy to overcome this problem; it was only possible to sample between one and three ignimbrite units or lava flows at any locality (Table 3). Paleomagnetic data from different sites were grouped

to determine a mean orientation (Table 4). Given enough sites, this mean direction should contain information about large-scale vertical axis rotations (Table 4).

The kilometer-scale dimensions of medium- to coarse-grained intermediate intrusive bodies sampled in this study suggest that cooling was on a timescale of  $\sim 10^4$  to  $10^5$  years. The Comanche intrusion (COM in Table 3) outcrops in a roughly equidimensional region nearly a kilometer across; the Mina Cunurana body (MC in Table 3) is several kilometers across. If magnetization was acquired progressively during cooling of the intrusion below the Curie temperature of the magnetic carriers, mirroring the range of unblocking temperatures revealed by laboratory thermal demagnetization, then, given the cooling timescale, it is possible that the magnetization in individual samples or even specimens has averaged out the effects of paleosecular variation [Butler, 1992]. In this study, the question of the tectonic significance of the magnetizations in these intrusions is left open, except that the mean magnetization for the Mina Cunurana body is included in a grouping of volcanic sites (Table 4).

**4.3.3. Dispersion.** Paleosecular variation gives rise to dispersion of the virtual geomagnetic poles calculated from individual site magnetizations. The magnetostratigraphic study of middle Miocene red beds in the Bolivian Altiplano [Roperch *et al.*, 1999]

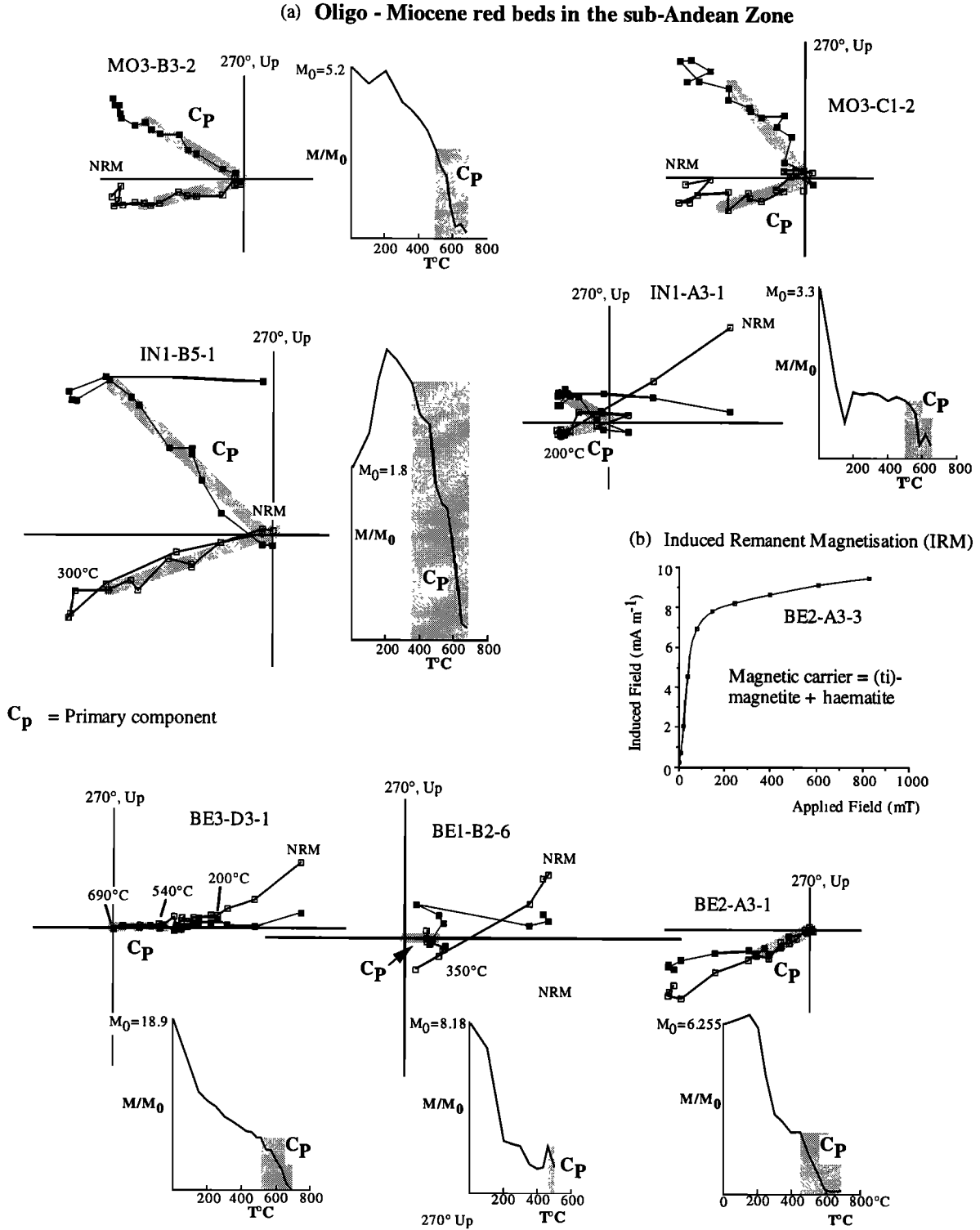


**Figure 12.** Demagnetization data (Zijderveld plots, total magnetization intensity plots, and equal-area stereonets) for Oligo-Miocene red beds from the western margin of the sub-Andean zone (see Figures 2, 6 and 8c). Solid circles on stereonets denote positive inclinations; open circles show negative inclinations. (a) Generally, two components defined during stepwise thermal demagnetization: (1) a low unblocking temperature component, with normal polarity, which sometimes persists up to 200°C and (2) a higher unblocking temperature reversed or normal polarity component which is often not completely removed below 650°C, referred to as  $C_p$  and shaded. This suggests that both (ti)-magnetite and hematite are important magnetic carriers. Specimens MO3-B3-2, IN1-B5-1, and BE2-A3-1 show well-defined reversed polarity  $C_p$  components; BE3-D3-1 is normal polarity. Specimen MO3-C1-2 shows a "noisy" reversed polarity  $C_p$  component, while IN1-A3-1 has a typical "stalled" demagnetization pattern suggesting hematite is the main magnetic carrier here (see text). (b) IRM studies suggest (ti)-magnetite and haematite as the magnetic carriers.

Table 2. Paleomagnetic Data for Oligo-Miocene Red Sandstones and Siltstones in the Sub-Andean Zone Analyzed in This Study

Locality	Label	Lat°S/Long°W	Age, Ma	Lithology/ Stratigraphy <sup>a</sup>	N <sup>b</sup>	D <sup>c</sup>	I <sup>d</sup>	α <sub>95</sub> <sup>e</sup>	k <sup>f</sup>	σ <sup>g</sup>	Bedding	Corr. D <sup>c</sup>	Corr. I <sup>d</sup>	R±AR <sup>d</sup>	F±AF <sup>d</sup>
Monteagudo 1	MO1	19.9/63.95	25±5	fs+silt/50 m	8/5	019	-10	7	56	12	350/60E	356°	-30°	-3±8	-8±7
Monteagudo 2 <sup>f</sup>	MO2	19.95/63.9	25±5	fs+silt/1.5 m	17/14	196	-11	3	137	7	322/45E	192°	25°	(13±5)	(-18±5)
Monteagudo 3 <sup>f</sup>	MO3	20.0/63.9	25±5	fs+silt/7 m	9/9	204	17	7	50	12	354/44E	183°	33°	(4±8)	(-10±7)
Ingre1	IN1	20.7/63.85	25±5	fs+silt/12 m	11/11	219	13	7	46	14	007/70E	184°	34°	5±8	-10±7
Ingre2 <sup>f</sup>	IN2	20.73/63.85	25±5	fs+silt/3.5 m	12/12	336	-8	7	35	15	194/90W	024°	-37°	(25±8)	(-7±7)
Ingre3	IN3	20.75/63.85	25±5	fs+silt/50 m	13/6	032	-8	11	15	23	009/85E	003°	-23°	4±11	-21±10
Rio Salado 2	SAL2	21.25/64.15	25±5	fs+silt/35 m	12/6	164	23	12	15	24	175/50W-48E	172°	28°	-7±12	-16±11
Rio Salado 3 <sup>h</sup>	SAL3	21.25/64.4	25±5	fs+silt/100 m	15/6	339	1	6	28	18	182/54W	188°	35°	9±13	-9±11
Bermejo 1	BE1	22.4/64.45	25±5	fs+silt/100 m	23/12	155	24	6	28	18	208/90W	033°	-53°	34±9	7±7
Bermejo 2 <sup>f</sup>	BE2	22.43/64.47	25±5	fs+silt/4.5 m	8/8	163	22	5	121	8	204/86W	227°	38°	(48±7)	(-8±6)
Bermejo 3	BE3	22.45/65.0	25±5	fs+silt/115 m	14/14	346	-5	8	23	18	205/80W	023°	-40°	24±10	-6±8

<sup>a</sup> Lithology (fs, fine sandstone, silt, siltstone), sampled stratigraphic thickness in metres.  
<sup>b</sup> Number of specimens and samples (see text).  
<sup>c</sup> D, declination; I, inclination; α<sub>95</sub>, 95% angular confidence limit; k, Fisher precision parameter, σ, angular dispersion; Corr D and Corr I are tilt corrected  
<sup>d</sup> R±AR, vertical axis rotation and standard error, F±AF, flattening and standard error, calculated with respect to *Randall* [1998] Neogene South American reference paleomagnetic pole, using the method of *Butler* [1992]. Values in parentheses are for localities with a stratigraphic thickness < 10m  
<sup>e</sup> Magnetizations are constrained by tilt or fold tests to have occurred after tectonic tilting.  
<sup>f</sup> Localities have stratigraphic thicknesses < 10 m, and paleosecular variation may not be averaged (see text)  
<sup>g</sup> Great circle analysis used to determine mean magnetisation

Table 3. Paleomagnetic Data for Miocene Volcanic Rocks and Intrusions in the Altiplano and Eastern Cordillera Analysed in this Study

Site or Locality	Label	Lat°S/Long°W	Age, Ma <sup>a</sup>	Scale <sup>b</sup>	N <sup>b</sup>	D <sup>c</sup>	I <sup>d</sup>	α <sub>95</sub> <sup>e</sup>	k <sup>f</sup>	σ <sup>g</sup>	Bedding	Corr. D <sup>c</sup>	Corr. I <sup>d</sup>	Comments <sup>d</sup>
Comanche	COM	16.9/68.4	14±2	hundreds of meters	22/11	297	-19	9	25	25	161/25W	307	-35	mg intermediate intrusion + xenoliths (GC)
Comanche	COM	16.9/68.4	14±2	hundreds of meters	10/6	306	-24	5	9	18	161/25W	318	-36	mg intrusion only (GC)
Comanche	COM	16.9/68.4	14±2	hundreds of meters	13/5	296	-27	11	15	24	161/25W	308	-42	mafic xenoliths only
Tres Monos lavas	OLI-3	21.1/68.4	8.5±1	>>5 m	16/16	019	-37	12	11	29	No tilt			one or more andesitic lava flows
Tambo Tambillo	CHIAR	19.45/67.35	24±2	35 m	3/1	047	-10	2	4031	2	002/67E	011	-45	fg mafic sill
Mina Cururana	MC	19.8/65.7	24±2	-1 km	7/4	173	62	8	65	14	7096/25S <sup>h</sup>	179°	37°	cg felsic intrusion
Mina Japo	JAP	18/66.8	7±1	>5 m	4/3	175	11	8	125	9	No tilt			single flow
Huanuni	HUA	18.2/66.75	7±1	>5 m	11/10	163	31	6	70	12	No tilt			single flow
Tingupaya Road	TR	19.3/66	7±1	>10 m	10/6	015	-46	2	419	4	No tilt			single flow
Uyuni Road	POR	19.71/65.87	12±1	>5 m	9/5	184	21	2	986	3	No tilt			single flow
Yonsa Peninsula	YON	20.35/67.95	14±2	-5 m	6/6	018	-49	11	41	17	198/20W	040	-45	single flow
Tahua Formation	TAHI	19.85/67.75	14±2	-5 m	8/4	163	35	2	591	2	218/23W	178	52	single flow
Tahua Formation	TAHI-3	19.85/67.75	14±2	3 x -5 m	15/8	346	-32	20	46	46	218/23W	000	-49	three flows (G.C)

<sup>a</sup> Thickness or characteristic dimension of rock body  
<sup>b</sup> Number of specimens and samples.  
<sup>c</sup> D, declination; I, inclination; α<sub>95</sub>, 95% angular confidence limit; k, Fisher precision parameter, σ, angular dispersion; Corr D and Corr I are tilt corrected.  
<sup>d</sup> GC, great circle analysis (see Fig 1.3), cg, mg, fg, are coarse, medium, fine grained, respectively.  
<sup>e</sup> Tilt correction based on structure of Paleozoic country rock strata

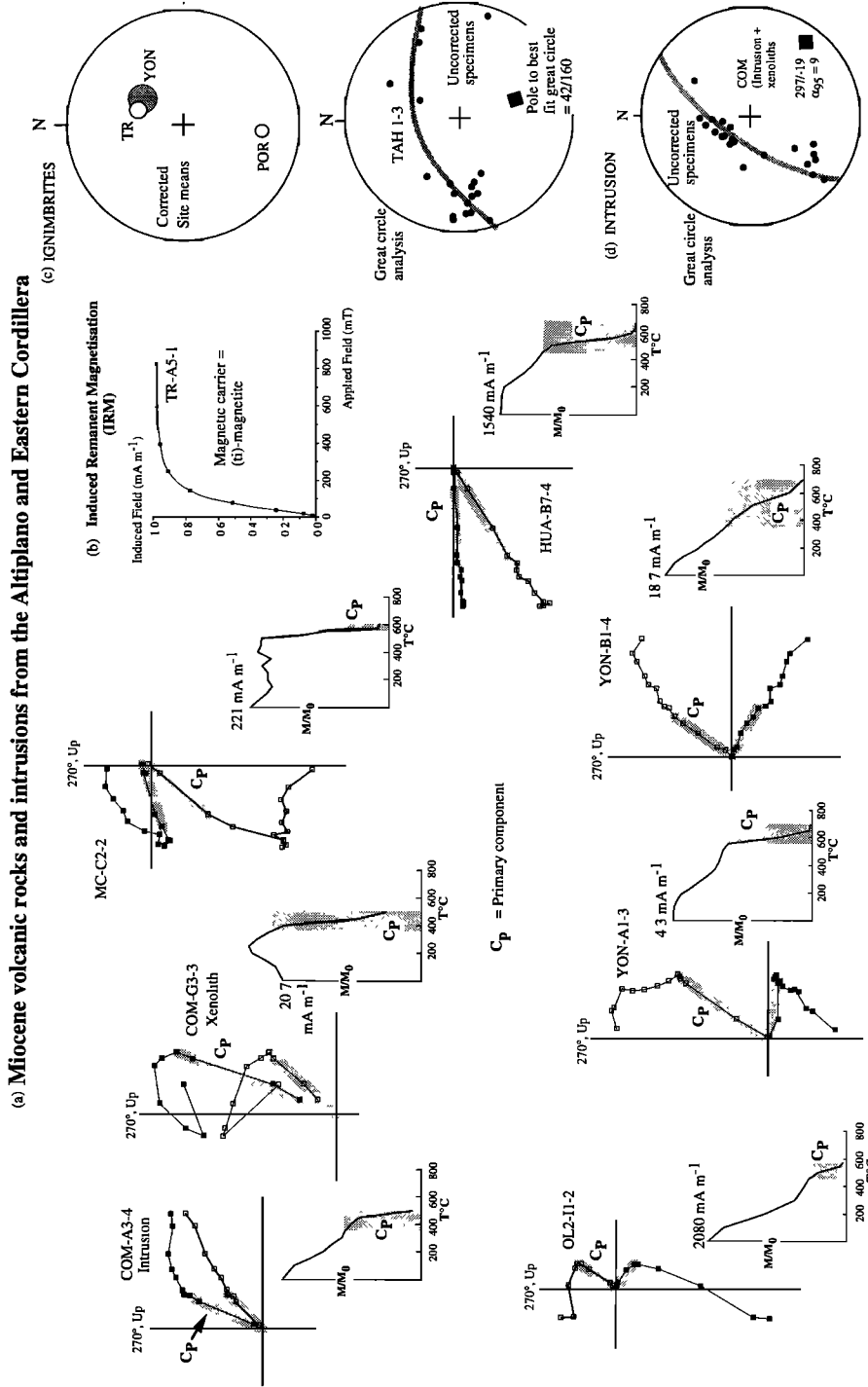
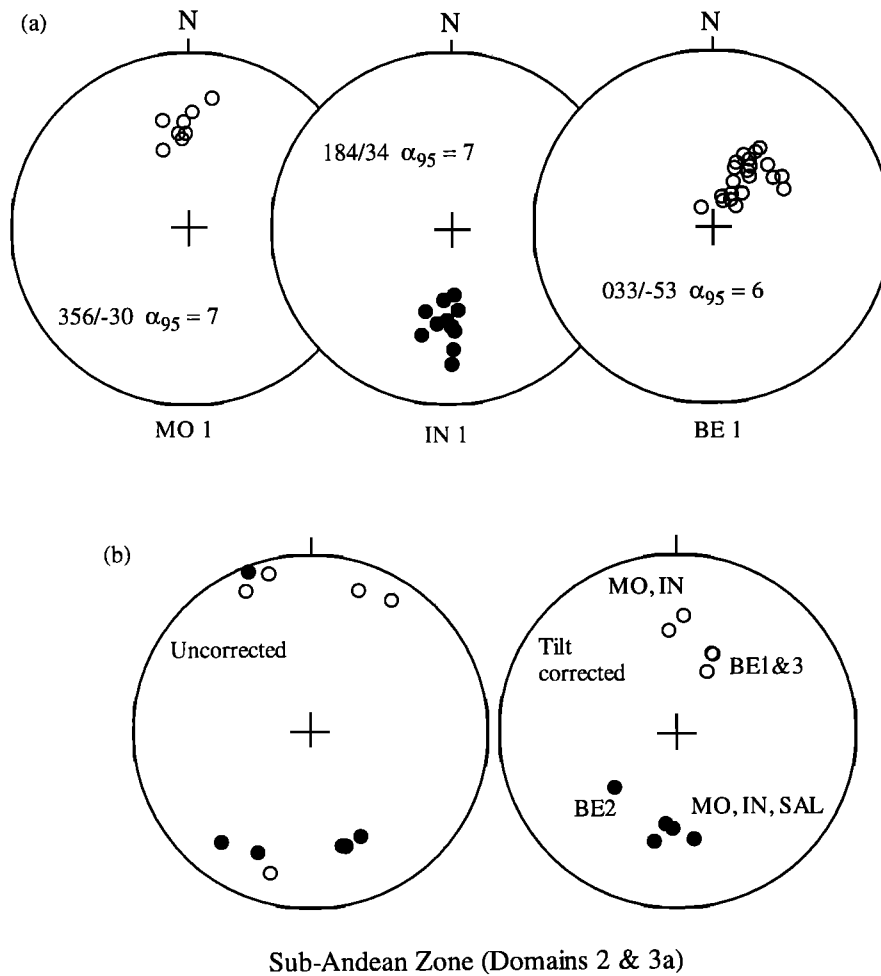


**Figure 13.** Demagnetization data (Zijderveld plots, total magnetization intensity plots, and equal-area stereonets) for Miocene volcanics and intrusions from the Altiplano and Eastern Cordillera (see Figures 2, 8d, and Table 3 and caption to Figure 9). Solid circles on stereonets denote positive inclinations; open circles show negative inclinations. (a) All specimens illustrated showing well defined normal or reversed polarity high unblocking temperature components (labeled  $C_p$  with shading), unblocked between  $\sim 350^\circ\text{C}$  and  $600^\circ\text{C}$ . This suggests the magnetic carrier in all cases is (Ti)-magnetite. (b) (Ti)-magnetite magnetic carrier confirmed by IRM studies, which show rapid acquisition for applied fields up to 300 mT, with saturation for higher applied field strengths. (c) – (d) Stereonet plots of site means for three middle to upper Miocene ignimbrites (TR, POR, YON) and great circle plots for TAHI-3 ignimbrites and COM dioritic intrusion and xenoliths, which have overlapping blocking spectra with curved unblocking trajectories on Zijderveld plots. The pole of the best fit great circle is an estimate of the primary magnetic component.



## Sub-Andean Zone (Domains 2 &amp; 3a)

**Figure 14.** Equal area stereonet plots showing high unblocking temperature reversed and normal polarity components ( $C_p$  in Figure 11) for Oligo-Miocene red beds on the western margin of the sub-Andean (Table 2, and Figures 2 and 6). Solid dots denote positive inclinations; open circles show negative inclinations. Stereonet plots are shown (a) for specimen magnetizations in individual localities (after tilt correction) and (b) for different localities before and after tilt correction.

**Table 4.** Paleomagnetic Data for Grouped Sites or Localities in This Study

Grouped Sites/Localities <sup>a</sup>	Lat °S/Long. °W	Age Ma	$N^c$	$D$	$I$	$\alpha_{95}$	$R \pm \Delta R^b$	$F \pm \Delta F^b$
<i>Sites in Altiplano and Western Margin of Eastern Cordillera (Domain 2)</i>								
TR+POR+YON+TAH1+TAH 1-3+OLI-3	19 4-20.9/66-69	7-14	6	012	-43	14	14±16	0±11
TR+POR+YON+TAH1+TAH 1-3 OLI-3+CHIAR+MC	19 3-20 9/65.8-69	7-24	8	010	-42	10	12±12	-1±9
<i>Localities in Eastern Cordillera</i>								
<b>Cochabamba (Domain 3b)</b>								
LC+SAN+SAY+ CAP	17 4-17.7/66.3-66.6	65±5	4	204	48	12	32±15	6±10
<b>Otavi Syncline (Domain 2)</b>								
OTA+CANI+CAN2	20/65 3	80±5	3	170	48	15	1±18	7±12
<b>Camargo Syncline (Domain 2)</b>								
CHA+ SAR + VIN	20 6/65 2	65±5	3	189	49	14	17±18	3±12
(PAL+TUM+ELP+CAZ) <sup>e</sup>	20.7-21.4/65 2	?65±5	4	196	42	11	24±12 <sup>c</sup>	-4±10 <sup>c</sup>
(VIN+PAL+TUM+ELP+CAZ+TOJO) <sup>d</sup>	20 7-22.8/65.25	?Neogene	6	182	42	4	3±6 <sup>d</sup>	-2±5 <sup>d</sup>
<i>Localities in Sub-Andean Zone (Domains 2 and 3a)</i>								
MO 1-3	19.95/63 9	20-30	3	184	30	12	5±12	-13±11
IN 1-3	20 73/63 85	20-30	3	010	-33	22	11±22	-11±18
MO 1-3 + IN 1-3	19 9-20.8/63.9	20-30	6	187	31	9	8±10	-12±8
MO 1-3 + IN 1-3 + SAL 2-3 (Domain 2)	19 9-21.2/63.8-64.1	20-30	8	185	32	7	6±8	-12±7
BE 1-3 (Domain 3a)	22 4/64.5	20-30	3	035	-44	19	36±22	-2±16

<sup>a</sup> Sites or localities listed in Tables 1 to 3

<sup>b</sup>  $R \pm \Delta R$ , vertical axis rotation and standard error;  $F \pm \Delta F$ , flattening and standard error, calculated with respect to *Randall's* [1998] Neogene or *Roperch and Carlier's* [1992] 60 and 80 Ma South American reference paleomagnetic poles, using the method of *Butler* [1992]

<sup>c</sup> Age of magnetization uncertain;  $R \pm \Delta R$  calculated assuming magnetization acquired before tilting at 65±5 Ma

<sup>d</sup> Age of magnetization uncertain;  $R \pm \Delta R$  calculated assuming magnetization acquired after tilting during Neogene.

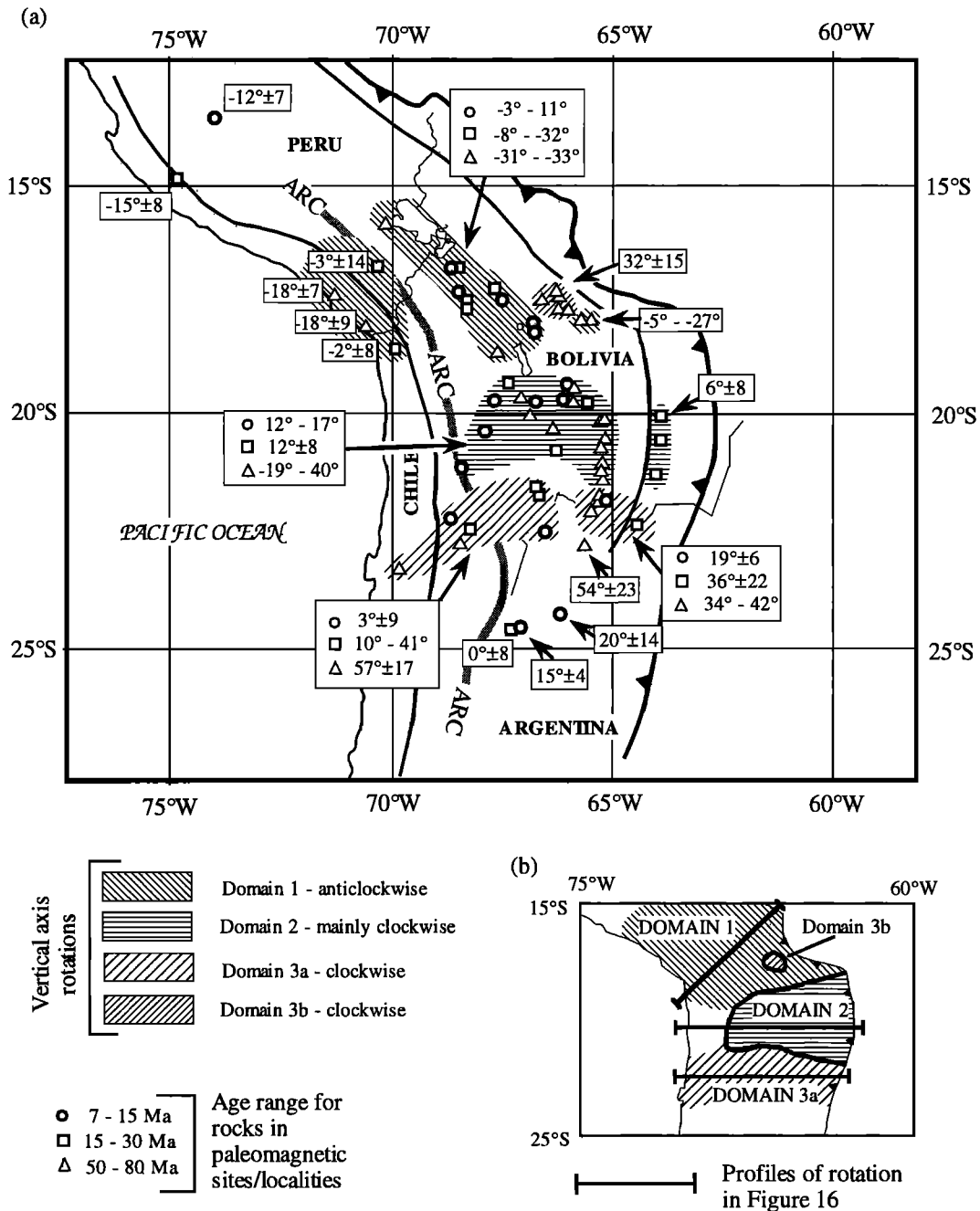


**Figure 15.** (a) Map of the Andes in Bolivia, northern Chile, northern Argentina, and Peru, showing the general topographic and tectonic trends in the Bolivian orocline. A summary is given of rigid body vertical axis rotations deduced from paleomagnetic measurements for rocks younger than 80 Myr, based on this study and published work (see Tables 1-6). (b) The pattern of vertical axis rotations for rocks in the age range 20-80 Ma defines three regional domains in the Bolivian Andes. Crustal blocks in domain 1, on the northern flank of the Bolivian orocline, have undergone an anticlockwise rotation about a vertical axis in the range  $\sim 8$  to  $\sim 33^\circ$ ; blocks from domain 2 immediately south of the main oroclinal bend have rotated between  $\sim 19^\circ$  anticlockwise and  $\sim 40^\circ$  clockwise. Even farther south, in domain 3b, blocks have rotated between  $\sim 3^\circ$  and  $\sim 57^\circ$  clockwise. A localized area (domain 3b), in which blocks have undergone  $\sim 32^\circ$  clockwise rotation in the last  $\sim 65$  Myr, lies within the southeastern part of domain 1. The northern boundary of domain 1 and the southern boundary of domain 3a are as yet not well defined. Also shown are the lines of profiles across each domain, which have been used to determine the distribution of rotation across the width of the Andes (see Figure 16).

provides the best available local estimate of this dispersion; the standard error ( $\sim 2.5^\circ$ ) of the mean magnetization (with an inclination of  $\sim 22^\circ$ ) for 79 site measurements of magnetization over a stratigraphic thickness of  $\sim 5$  km suggests a dispersion of  $\sim 13^\circ$ . This dispersion is slightly less than the  $\sim 19^\circ$  predicted from global studies of Miocene to Eocene rocks [Butler, 1992].

Dispersion for localities in this study are generally in the range  $9^\circ$  to  $30^\circ$ , with a geometric mean of  $15^\circ$  (Tables 1-3). This suggests that, in general, the observed dispersion is consistent with that expected from paleosecular variation. The higher values probably reflect "noise" associated with the complex magnetic behavior of the magnetic carriers during demagnetization, giving

**Table 5.** McElhinny Fold Tests for Paleomagnetic Samples or Localities in This Study

Localities	Number of Sample/ Localities	$k_1^*$ , Without Tilt Correction	$k_2^*$ , With Tilt Correction	$k_2/k_1$	Passed Test at 99% Confidence Level
Domain 3b (LC, SAN, CAP, SAY)	/4	3.3	61.2	18.5	Yes
Domain 2, 3a (MON, ING, SAL, BER)	/11	8.8	27.1	3.1	Yes
Domain 2 (MON, ING, SAL)	/8	8.6	63.6	7.4	Yes
Domain 2 (CHA, SAR, VIN)	24/	4.8	32.8	6.8	Yes
Domain 2 (OTA, CANI, CAN2)	22/12	2.5	38.0	15.3	Yes

\* Fisher precision parameter.

rise to incomplete characterization of the individual magnetic components. The smaller dispersions, particularly for the limestone localities, may be a consequence of the magnetization in individual samples or specimens being acquired over long periods, effectively damping the observed magnetic variation within a locality [Butler, 1992]. This might be expected for bioturbated and well-cemented limestones, where the acquisition of magnetization clearly occurred during or after diagenesis, very likely over a protracted period. The low dispersion of  $8^\circ - 9^\circ$  for two localities in Oligo-Miocene red beds (Table 2, localities MO2 and BE2), where a very limited stratigraphic sequence was sampled, could be because paleosecular was not completely averaged and/or there has been considerably "smoothing" as a consequence of bioturbation and diagenesis during lithification [Butler, 1992].

#### 4.4. South American Paleomagnetic Reference Poles

The direction of the locality mean primary magnetization can be used to calculate a mean geomagnetic pole, given the locality position and assuming a geocentric axial dipolar magnetic field at the time of acquisition [Butler, 1992]. In the absence of any plate motion, or deformation other than local tilting, this pole should coincide with either the north (normal magnetization) or south

(reversed magnetization) geographic poles. To separate out the effects of local deformation from large-scale plate motion, it is necessary to determine reference paleomagnetic poles that reflect plate motions since the locality magnetization was acquired. As the localities described above are in rocks that lie on the western margin of the South American plate, it is the motion of this plate that is of most interest in this study. In this case, South America forms the reference frame, and all motions detected paleomagnetically are in relation to this reference frame.

Relevant reference paleomagnetic poles for the South American plate are for the period between 80 Ma and 7 Ma. Various authors [Randall, 1998, and references therein; Roperch and Carlier, 1992] have determined paleomagnetic poles for South America in this time frame, on the basis of paleomagnetic studies of rocks on the stable South American plate, and also data from Africa rotated into the South American reference frame. In this study, I use the average Neogene paleomagnetic pole derived by Randall [1998] for the 7-25 Ma period and the reference poles derived by Roperch and Carlier [1992] for older time periods. The reference paleomagnetic pole for the Neogene is within  $5^\circ$  of the present geographical poles, while Paleogene to Cretaceous reference poles (30-80 Ma) are within  $10^\circ$  of the geographical poles.

**Table 6.** Published Paleomagnetic Data for Upper Cretaceous to Miocene Rocks Between  $\sim 13^\circ\text{S}$  and  $25^\circ\text{S}$ 

Name	Label	Lat°S/Long°W	Age, Ma	$D^a$	$I^a$	$\alpha_{95}^a$	Declination Anomaly <sup>b</sup>	Reference
Ocos		13.4/74.0	2-24	346	-32	5	-12±7	Heki et al. [1985]
Nazca		14.8/74.7	19-22	163	25	7	-15±8	after Macedo-Sanchez et al. [1992]
Umayo		15.8/70.1	58-75	319	-24	10	-33±9	Butler et al. [1995]
Viacha		16.8/68.5	25-35	169	32	11	-12±11	Roperch et al. [2000]
Salla		17.2/67.7	24-28	353	-37	5	-8±6	MacFadden et al. [1990]
Micana		17.5/67.5	6.5-7.5	355	-26	6	-3±6	MacFadden et al. [1990]
Chuquichambi (N)		17.5/68.3	25-35	329	-27	8	-32±7	Roperch et al. [2000]
Chuquichambi (S)		17.5/68.3	25-35	340	-30	16	-21±15	Roperch et al. [2000]
Totora Fm		17.5/68.3	9-15	347	-22	3	-11±4	Roperch et al. [1999]
Ilo, Peru		17.5/71.4	~80	331	-40	9	-18±9	Roperch and Carlier [1992]
Tiupampa	TIU	18.0/65.5	58-66	347	-38	8	-5±9	Butler et al. [1995]
Sucusuma	SUC	18.1/65.8	58-66	325	-47	5	-27±7	Butler et al. [1995]
La Yarada		18.1/70.7	~80	331	-38	6	-18±7	Roperch and Carlier [1992]
Anca		18.5/70	~19	358	-34	8	0±9	Roperch et al. [2000]
La Palca	PALC	19.5/65.9	64-75	033	-42	4	40±12	Butler et al. [1995]
Quehua	QUEHA	20.0/67.0	7-13	015	-38	9	17±10	MacFadden et al. [1995]
Cerdas	CERD	20.8/66.3	15.5-16.5	010	-39	7	12±8	MacFadden et al. [1995]
Lipez1		21.7/66.6	~20	218	39	11	41±13	Roperch et al. [2000]
Lipez2		21.7/66.6	~20	188	45	15	10±18	Roperch et al. [2000]
Quebrada Honda	HONDA	22.0/65.5	12-13	018	-41	4	19±6	MacFadden et al. [1990]
Yavi		22.2/65.5	~80	022	-22	12	34±11	Coutand et al. [1999]
El Loa		22.3/68.6	11.3	001	-46	7	3±9	Somoza et al. [1999]
Granada		22.6/66.5	~9	181	31	7	3±8	after Somoza et al. [1996]
Paciencia Group		22.6/68.3	~20	020	-27	14	22±13	Hartley et al. [1992]
Purnilactis Fm		22.8/68.4	58-98	041	-36	9	53±9	Hartley et al. [1992]
Abra Pampa		22.8/65.7	~80	042	-48	19	54±23	Coutand et al. [1999]
Baquadano region		23.4/69.8	24-66	056	-41	9	57±17	Dupont-Nivet et al. [1996]
Salar de Arizaro 1		24.6/67.3	~30	001	-35	8	0±8	Coutand et al. [1999]
Salar de Arizaro 2		24.6/67.2	~10	012	-39	3	15±4	Coutand et al. [1999]

<sup>a</sup>  $D$ , declination,  $I$ , inclination,  $\alpha_{95}$ , 95% angular confidence limit.

<sup>b</sup> Calculated with respect to Randall [1998] Neogene or Roperch and Carlier [1992] 30, 60, and 80 Ma South American reference paleomagnetic pole, using the method of Butler [1992]

In many cases, the poles determined for an individual locality or group of localities, in this study, are significantly different at the 95% confidence level to the relevant South American reference paleomagnetic pole (Tables 1, 2, and 4). These discrepancies are described in terms of declination ( $R$ ) and inclination ( $F$ ) anomalies, with their associated 95% confidence limits.

#### 4.5. Declination Anomalies

If the mean magnetization for a locality is representative of the Earth's geocentric axial dipole field at the time of acquisition, then declination anomalies ( $R$ ) can be interpreted to be the result of displacement of the locality since the acquisition of the magnetization. The displacement of the locality can be thought of as a translation relative to the South American plate, as a consequence of tectonic shortening, together with a rigid body rotation about a vertical axis which passes through the locality. Where there is a significant possibility, as has already been discussed, that the mean locality magnetization determined in this study does not average paleosecular variation ( $R$  shown in parentheses in Tables 1

and 2), then only the declination anomalies for groupings of neighboring localities or sites are considered (Table 4).

Paleomagnetic localities in the Bolivian Andes have been translated between 100 km and 300 km in an approximately ENE direction toward the South American plate during the Cenozoic [Kley and Monaldi, 1998], whereas the calculated declination anomalies imply vertical axis rotations for localities or appropriate groupings of localities or sites in the range  $\sim 42^\circ$  clockwise to  $\sim 31^\circ$  anticlockwise. Many of the rotations are  $< 20^\circ$  and are in good agreement with previous studies (see below). The relatively small magnitudes of the rotations highlight the importance of the choice of reference poles. However, relative rotations between adjacent regions can be determined for localities with rocks of the same age, independent of the reference poles.

Relative vertical axis rotations determined in this study for locations along the western margin of the sub-Andean zone, and some fold structures in the Eastern Cordillera and Altiplano, correlate well with swings in the structural trend (see below). These correlations provide further support for the use of declination anomalies, calculated from the appropriately grouped paleomagnetic measurements in this study, as estimates of rigid body vertical axis rotations.

#### 4.6. Inclination Anomalies

In most cases, the observed mean inclination is not significantly different from the expected inclination at the 95% confidence level, given the appropriate reference pole and sampling location, for groupings of localities (Table 4) and individual localities (Tables 1-3). The observed mean inclination anomalies,  $F$ , for individual localities are in the range  $-21^\circ$  to  $14^\circ$  (negative anomalies imply a shallower observed inclination than expected), with  $F$  usually  $\leq 0$ . The small latitudinal shifts during the Cenozoic of locations in the Bolivian Andes, in relation to stable South America as a consequence of Andean deformation [Lamb *et al.*, 1997; Lamb and Hoke, 1997], could only generate inclination anomalies

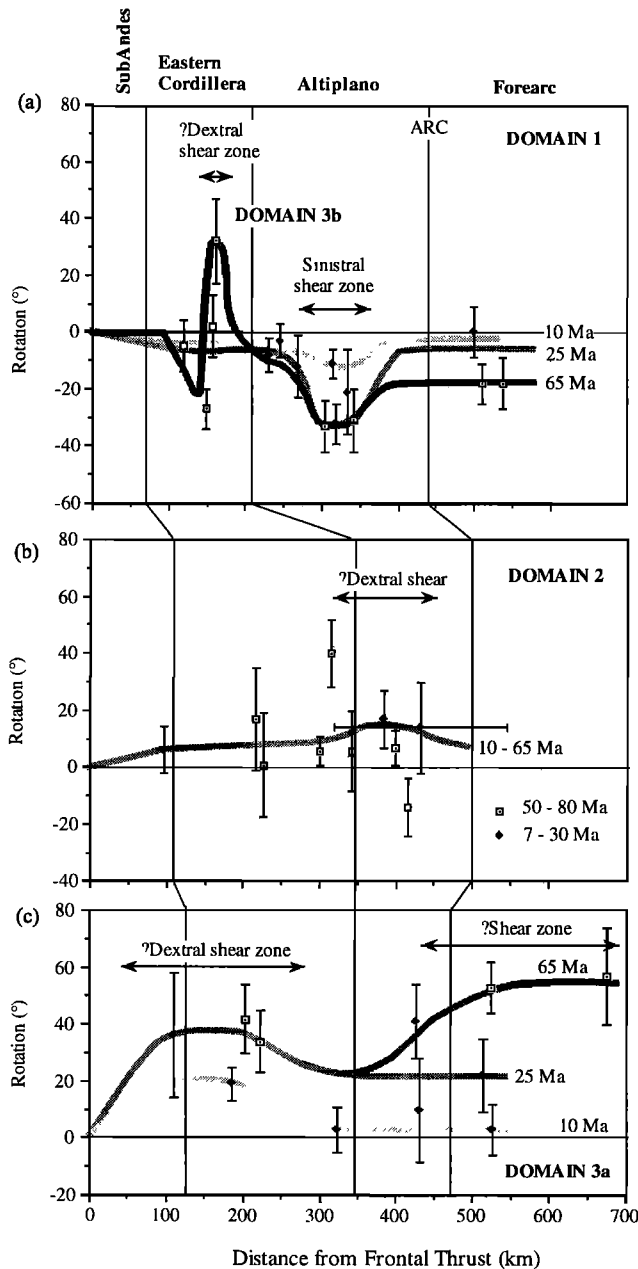


**Figure 16.** Plots showing the relation between paleomagnetically determined vertical axis rotations, relative to stable South America, and the geographical position of localities (projected on to profiles in Figure 15) for the domains defined in Figure 15. By definition, vertical axis rotation on the eastern margin of the sub-Andes is zero. Squares indicate rotations for 50-80 Ma rocks and diamonds are for 7-30 Ma rocks; curves illustrate inferred distribution of rotation for rocks with specific ages. (a) Profile in domain 1 also spanning domain 3b, giving rise to marked variation in the observed vertical axis rotation for rocks 60 Ma or older, ranging from strongly clockwise in the Eastern Cordillera to anticlockwise in the Altiplano and forearc. The data for younger rocks suggest enhanced anticlockwise rotation in the Altiplano in a zone of sinistral shear and only minor rotation in the forearc. (b) Profile in domain 2, where there is no clear systematic relation between vertical axis rotation and age of rocks, except that 50-80 Ma rocks have a marked scatter about a mean of  $\sim 8^\circ$  clockwise. There is a suggestion of slightly enhanced local clockwise vertical axis rotation in the Altiplano, compared to the Eastern Cordillera and sub-Andes. Otherwise, it appears that domain 2 has undergone a regional vertical axis clockwise rotation between  $5^\circ$  and  $10^\circ$  in the last  $\sim 10$  Myr. (c) Profile in domain 3a which has undergone clockwise vertical axis rotations in the range  $30^\circ$  to  $60^\circ$  in the last 65 Myr, with possibly slightly enhanced rotation in the Eastern Cordillera and forearc. However, the forearc and Altiplano appear to have undergone less than  $10^\circ$  vertical axis rotation in the last  $\sim 10$  Myr.

$\leq 2^\circ$ . Inclination flattening up to  $25^\circ$  has been commonly observed in previous studies on sedimentary sequences in the central Andes [Roperch *et al.*, 1999; Coutand *et al.*, 1999]. The most plausible explanation for the flattening is compaction of the sedimentary sequences during burial which should leave the declination unaffected [Tauxe and Kent, 1984; Arason and Levi, 1990].

The origin of the inclination steepening, observed in a few Upper Cretaceous limestone localities, is unclear but may be a consequence of either incomplete averaging of paleosecular variation or incomplete characterization of primary magnetizations. Positive inclination anomalies, significant at the 95% confidence level, were only calculated for a few localities but never for the appropriate locality groupings (Table 4) used in this study for tectonic analysis.

## 5. Distribution and Timing of Vertical Axis Rotation

### 5.1. Domains of Vertical Axis Rotation

Information about the timing of vertical axis rotation requires paleomagnetic sampling of rocks with a wide range of ages from a particular geographical position. Unfortunately, rocks with a range in ages are usually only found at widely separated localities. For this reason, any analysis of the timing of vertical axis rotation is best done in conjunction with a discussion of their spatial variation, using all the available paleomagnetic data. This study substantially increases the number of paleomagnetic localities in the Bolivian Andes, providing a better geographical coverage, especially in the Eastern Cordillera, and extending the age of magnetization back to the earliest Cenozoic over a wide region. The following discussion makes use of paleomagnetic measurements in the central Andes in Bolivia, northern Chile, southern Peru, and northwestern Argentina, based on this study (Figure 15 and Tables 1-4) and previous work (Figure 15 and Table 6).

If the magnitude and sense of vertical axis rotation for each locality are plotted with respect to location, regardless of age (Figure 15), a pattern emerges of domains spanning almost the entire width of the Andes. We can think of these domains in terms of (1) a regional background rotation; reflecting large-scale tectonic processes; (2) the effects of more local deformation, adding a scatter to the paleomagnetic declination anomalies on top of the regional background rotation; and (3) a decreasing amount of rotation in younger rocks, reflecting a history of rotation during the Neogene. The magnitude of rotations observed in Upper Cretaceous-Paleocene limestones, outcropping throughout the Eastern Cordillera, show a particularly marked variation [cf. Butler *et al.*, 1995], even in localities only several kilometers apart (Figures 5 and 7).

The differences between the various domains is best seen in rocks in the age range  $\sim 20$  to 80 Ma; younger rocks acquired their primary magnetization at late stages in the vertical axis rotation history. For rocks older than 20 Ma, crustal blocks in domain 1, on the northern flank of the Bolivian orocline, have undergone an anticlockwise rotation about a vertical axis in the range  $\sim 8$  to  $\sim 33^\circ$ , with a geometric mean of  $\sim 22^\circ$ ; blocks from domain 2 immediately south of the main oroclinal bend have rotated between  $\sim 19^\circ$  anticlockwise and  $\sim 40^\circ$  clockwise, with a geometric mean of  $\sim 8^\circ$  clockwise. Even farther south, in domain 3b, blocks have rotated between  $\sim 10^\circ$  and  $\sim 57^\circ$  clockwise, with a geometric mean of  $37^\circ$ . A localized area (domain 3b), in which blocks have undergone  $\sim 32^\circ$  clockwise rotation in the last  $\sim 65$  Myr, lies within the southeastern part of domain 1. The northern boundary of domain

1 and the southern boundary of domain 3a are as yet not well defined.

### 5.2. Profiles of Vertical Axis Rotation

The relation between geographical position and vertical axis rotation within each domain can be examined by projecting the observed declinations anomalies for any particular locality or grouping of localities on to profiles which traverse the various rotation domains (Figure 16). By definition, the rotation must be zero on the eastern margin of the sub-Andean zone. It is clear that all the domains exhibit a variation in the magnitude of vertical axis rotation along the length of the traverses (inferred trends shown by various lines in Figure 16).

In domains 1 and 3b, 50 to 80 Ma rocks generally show the largest amount of rotation, ranging from  $\sim 32^\circ$  clockwise in the Eastern Cordillera to  $\sim 30^\circ$  anticlockwise in the Altiplano, decreasing to  $\sim 18^\circ$  anticlockwise in the Chilean forearc (Figure 16a). The pattern for younger rocks suggests a history of progressive rotation during the last  $\sim 25$  Myr, but with more rapid anticlockwise rotation in the Altiplano compared to either the Eastern Cordillera or the Chilean forearc region (Figure 16a). It appears that forearc rotation between  $\sim 16^\circ\text{S}$  and  $\sim 20^\circ\text{S}$  in the last  $\sim 20$  Myr has been much less than  $10^\circ$  anticlockwise [Roperch *et al.*, 2000] (Figure 16a); the magnitudes of forearc vertical axis rotation during the last  $\sim 20$  Myr appear to be significantly greater farther north, at  $\sim 15^\circ\text{S}$  (Figure 15, see below). The zones of enhanced clockwise (domain 3b) or anticlockwise rotation (Altiplano) in domain 1 may reflect rigid body rotations about a vertical axis in zones of shear, while the lower magnitudes of rotations elsewhere may reflect more regional bending of domain 1.

In domain 2 an underlying background rotation is apparent, which increases slightly from  $\sim 7^\circ$  clockwise on the western margin of the sub-Andes in  $\sim 25$  Ma red beds (though this rotation is not significant at the 95% confidence level) to possibly  $\sim 15^\circ$  clockwise in the Altiplano in  $\sim 10$  Ma red beds and volcanics. There are significantly larger clockwise rotations in domain 3a (Figure 16c), increasing from  $\sim 40^\circ$  on the western margin of the sub-Andean zone to over  $50^\circ$  clockwise in the forearc of northern Chile for 50-80 Ma rocks. Younger rocks in domain 3a show progressively smaller rotations (Figure 16c), with  $<10^\circ$  clockwise vertical axis rotation in the Altiplano and forearc for rocks  $\sim 11$  Ma and younger [Somoza *et al.*, 1996, 1999] but  $\sim 19^\circ$  clockwise for  $\sim 12$  Ma rocks in the Eastern Cordillera [MacFadden *et al.*, 1990].

### 5.3. Timing of Vertical Axis Rotation in Individual Domains

The timing of vertical axis rotation for individual domains can be investigated in greater detail by plotting the rotation for localities in each domain against the age of the rocks (Figure 17). In all domains, there is a considerable scatter of declination anomalies, especially for the older sample localities. It is clear from the previous analysis that the timing of rotation varies across the domains. Domain 2 displays the simplest rotation history (Figure 17b), with no clear evidence for a regional background rotation older than  $\sim 10$  Ma: a mean clockwise vertical axis rotation of  $\sim 8^\circ$  for 20-80 Ma rocks is not significantly different from the  $12^\circ \pm 12^\circ$  determined for a grouping of sites in 7-14 Ma volcanic rocks (this study, Table 4) and  $17^\circ \pm 10^\circ$  for 7-13 Ma red-beds (Table 6, locality Quehua, MacFadden *et al.* [1995]) outcropping in the Altiplano and western margin of the Eastern Cordillera. The wide variation in rotation for Upper Cretaceous to Paleocene rocks from different localities is likely to be a consequence of local rela-

tive vertical axis rotation over a longer period since the Eocene [cf. *Butler et al.*, 1995] when significant deformation in the Bolivian Andes was initiated [*Lamb et al.*, 1997; *Lamb and Hoke*, 1997].

The vertical axis rotation histories for domains 1, 3a, and 3b are complex (Figures 17a and c), with marked differences between the timing of rotation for crustal blocks in the Chilean forearc and Bolivian Altiplano, Eastern Cordillera, and sub-Andean zone. Postulated trends in the timing of rotation for the various physiographic provinces are shown in Figure 17. A general feature, already described, is the continued rapid rotation of crustal blocks in the Eastern Cordillera or Altiplano during the Neogene, while rotation in the forearc appears to be less than 10° either clockwise or anticlockwise [*Roperch et al.*, 2000; *Somoza et al.*, 1999].

#### 5.4. Vertical Axis Rotation and Structural Trends

**5.4.1. Upper Cretaceous–Paleocene rocks.** If the observed vertical axis rotations (this study) in Upper Cretaceous–Paleocene sedimentary rocks are plotted against the strike of the beds, regardless of dip (both westerly and easterly directions of dip) and excluding domain 3b, then a clear linear relation is observed (Figure 18a). Zero rotation corresponds to a strike of  $\sim 342^\circ$ , which is essentially orthogonal to both the axis of symmetry of the Bolivian orocline and also the average plate convergence vector during the Cenozoic ( $\sim 075^\circ$  [*Pardo Casas and Molnar*, 1987]). Anticlockwise rotations are observed in NW–NNW striking units, and clockwise rotation in N–NE striking units (Figure 18a). The slope of the best fit line is  $\sim 0.49$ , indicating that the overall strike variation is nearly twice as great as the observed range in vertical axis rotation (Figure 18a). This relationship is very similar to that obtained by *Coutand et al.* [1999] between the vertical axis rotation and the azimuth of anisotropy of magnetic susceptibility, which often correlates with tectonic fabric, for rocks in the Puna of northernmost Argentina, immediately south of the Bolivian Andes. This suggests that vertical axis rotation postdates or is synchronous with much of the folding, though on average about half the strike variation may reflect an original sinuosity of fold axes unrelated to vertical axis rotation.

In some specific cases all the sinuosity of a fold axial trace can be ascribed to vertical axis rotation. For instance, a pronounced  $\sim 025^\circ$  bend in the trend of a fold axial trace is clearly mirrored in a  $26^\circ \pm 8^\circ$  relative paleomagnetically determined vertical axis rotation between localities Agua Dulce and Chita (Table 1 and Figures 7 and 8d, localities AD and BET). This kinking must be synchronous or postdate the main folding in this region (i.e. younger than  $\sim 16$  Ma [*Lamb and Hoke*, 1997]) but must predate the upper Miocene Quehúa Formation which is subhorizontal and unconformably overlies the folded sequence [*MacFadden et al.*, 1995]. The relative clockwise vertical axis rotation of  $34^\circ \pm 13^\circ$  between two localities along the length of the Miraflores syncline, NW of Potosí (localities TAR (Table 1, this study) and PALCA (Table 5,

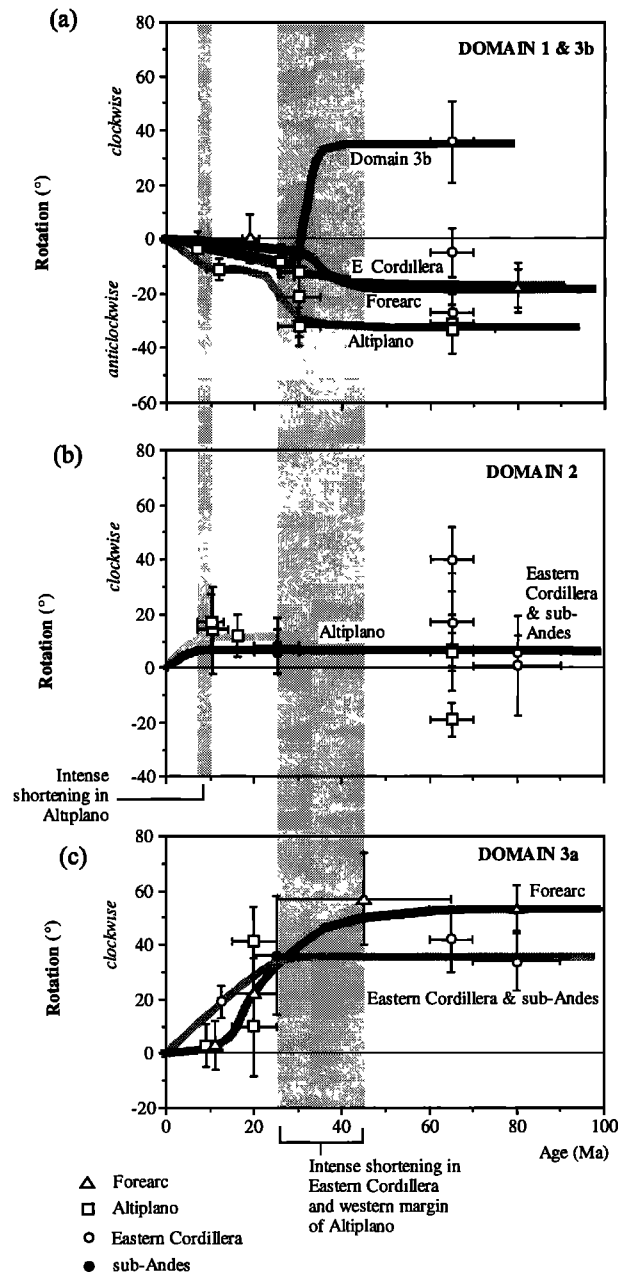


**Figure 17.** Plots showing the relation between paleomagnetically determined vertical axis rotations, relative to stable South America, and the stratigraphic or emplacement age of rocks, based on this study and published work (see Tables 1–4 and references therein). The data are plotted for the domains defined in Figure 15. Diamonds indicate rotations for rocks in the Altiplano; circles indicate rotations for rocks in the Eastern Cordillera and sub-Andes. There is considerable scatter in the data, especially for localities in Cretaceous rocks. Vertical axis rotations are interpreted in terms of (1) a regional vertical axis background rotation, and (2) a superimposed scatter which reflects more variable local rotation. Inferred background rotation histories for the different physiographic provinces are shown by curves. Integrating the rotation histories with the tectonic evolution of the Bolivian orocline suggests that Cenozoic vertical axis rotation in forearc commenced in the Eocene synchronous with the onset of crustal shortening in the Eastern Cordillera and Altiplano [*Lamb and Hoke*, 1997]. Neogene vertical axis rotation in the forearc has been generally small ( $<10^\circ$ ), whereas the Altiplano, Eastern Cordillera, and sub-Andes experienced significant Neogene vertical axis rotation. The onset of clockwise background rotation in domain 2 and local rotation in the Altiplano of domain 2 seem to coincide with intense shortening in both the Altiplano and sub-Andean zone at  $\sim 10$  Ma [*Lamb and Hoke*, 1997].

Butler *et al.* [1995]), coincides with  $\sim 30^\circ$  clockwise swing in the fold axial trace.

Clockwise vertical axis rotations, observed in upper Cretaceous-Paleocene limestones in domain 3b, deviate significantly from the overall linear relation with local strike (Figure 18a). The significance of this is unclear. One possibility is that the vertical axis rotations in domain 3b occurred before or early on in folding of the strata in this region. This way, there is no correlation between structural trend and rotation. In this case, the vertical axis

rotations here may be the earliest recorded in this part of the Bolivian Andes, of late Eocene-Oligocene age (i.e. 25-40 Ma [cf. Butler *et al.*, 1995]).

**5.4.2. Sub-Andean Oligo-Miocene red beds.** A plot of the vertical axis rotation of Oligo-Miocene red beds in the sub-Andean zone (domain 2), with the local strike of beds (for both westerly and easterly directions of dip), shows a clear 1:1 relation. The slope of the best fit line is  $\sim 1.02$  (Figure 18b). Zero vertical axis rotation corresponds to a strike azimuth of  $\sim 353^\circ$ , slightly different to that shown by Upper Cretaceous to Paleocene rocks (Figure 18b). The simplest interpretation is that the pronounced swing in structural trend of the sub-Andean zone in domains 2 and 3a is a consequence of bending during the last  $\sim 25$  Myr of an initially straight belt which trended  $\sim 353^\circ$ . The plot suggests a best fit  $\sim 7^\circ$  clockwise vertical axis rotation for rocks with an azimuth of  $\sim 000^\circ$ , corresponding to the mean structural trend in domain 2. This rotation is identical, within error, to that determined from a grouping of eight sub-Andean localities in domain 2 ( $6^\circ \pm 8^\circ$ , Table 4), but is based on data from 11 localities in domains 2 and 3a. It is also essentially the same as the mean vertical axis rotation in domain 2 ( $\sim 8^\circ$  clockwise) for rocks older than 20 Ma.

### 5.5. Vertical Axis Rotation and Topographic Trends

The most prominent feature of the Bolivian orocline is the swing in topographic trend from approximately NW north of the bend to more N-S farther south. The topographic expression of the Andes is widest in the bend region and becomes progressively narrower farther north and south. For this reason, the topographic trends of the eastern margin of the central Andes, in the sub-

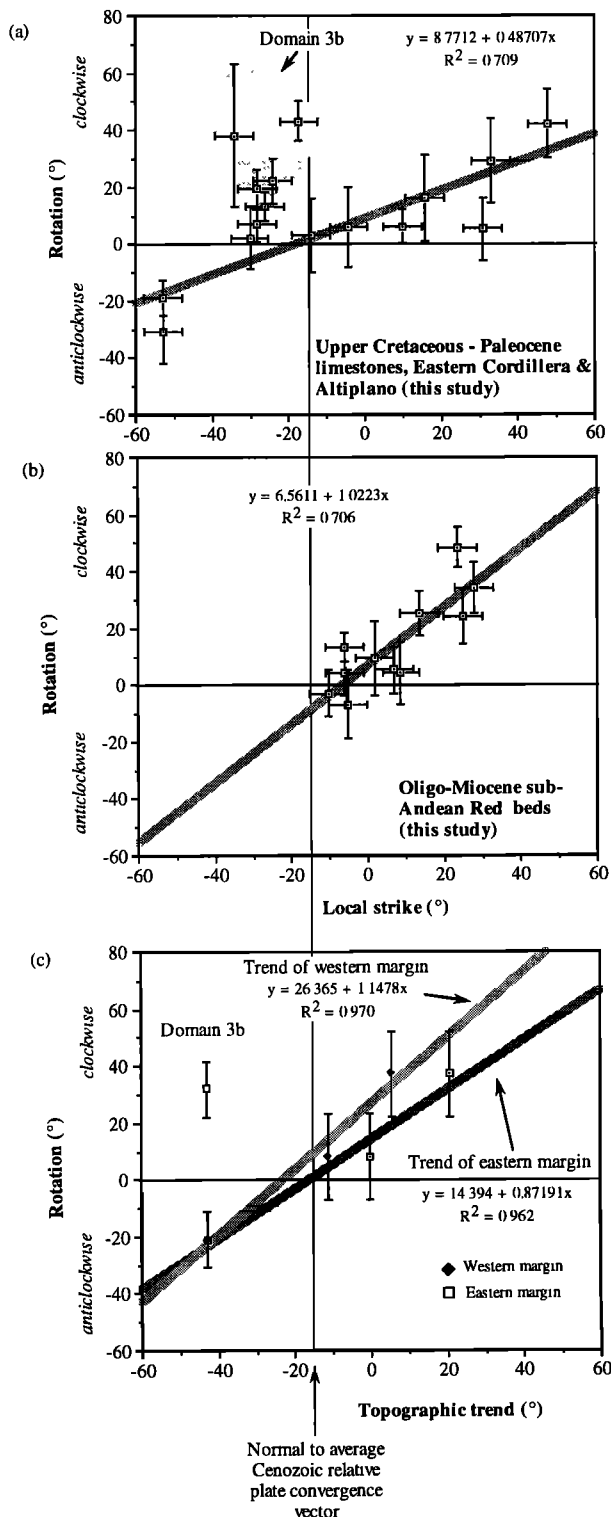


**Figure 18.** (a) Plot showing the relation between paleomagnetically determined vertical axis rotations in this study, relative to stable South America, and the strike of strata for 60-80 Ma rocks (see Table 1). The strike is shown as an azimuth: east of north is positive, west of north is negative. There is a clear linear correlation between the data for all localities (except those in domain 3b); however, the spread of strikes is nearly twice as great as that for observed rotations. This suggests that about half the strike variation is unrelated to tectonic rotation and may reflect an original sinuosity in fold structures which has been amplified by subsequent tectonic rotation. The zero rotation point corresponds with a strike of  $\sim 342^\circ$  ( $-18^\circ$ ), which is essentially normal to the instantaneous and long-term Cenozoic plate convergence vector in this region [Pardo Casas and Molnar, 1987]. Rotations for rocks in domain 3b deviate significantly from this trend. (b) The structural trend of the sub-Andean zone plotted against the vertical axis rotations for Oligo-Miocene red beds in sub-Andean localities in domains 2 and 3a (localities MO1-3, IN1-3, SAL2-3, and BE1-3). There is a clear 1:1 correlation, and the zero rotation point corresponds to a strike of  $\sim 353^\circ$  ( $-7^\circ$ ). The simplest interpretation is that the curvature of the structural trend of the sub-Andes in domains 2 and 3a is a consequence of bending. (c) The topographic trend of the western and eastern margins (shown as a deviation from north) of the central Andes plotted against the mean vertical axis rotation (error bars at 1 sigma level) for rocks in the age range 20 to 80 Ma for the various domains defined in Figure 15. The plot (excluding domain 3b) for the western margin has a slope  $>1$ , and that for the eastern margin has a slope  $<1$ . A plot of the mean vertical axis rotations of the domains with the mean topographic trend (average of trends of western and eastern margins) would have a slope of  $\sim 1$ ; this may be a coincidence (see text). Rotations for rocks in domain 3b deviate significantly from these trends.

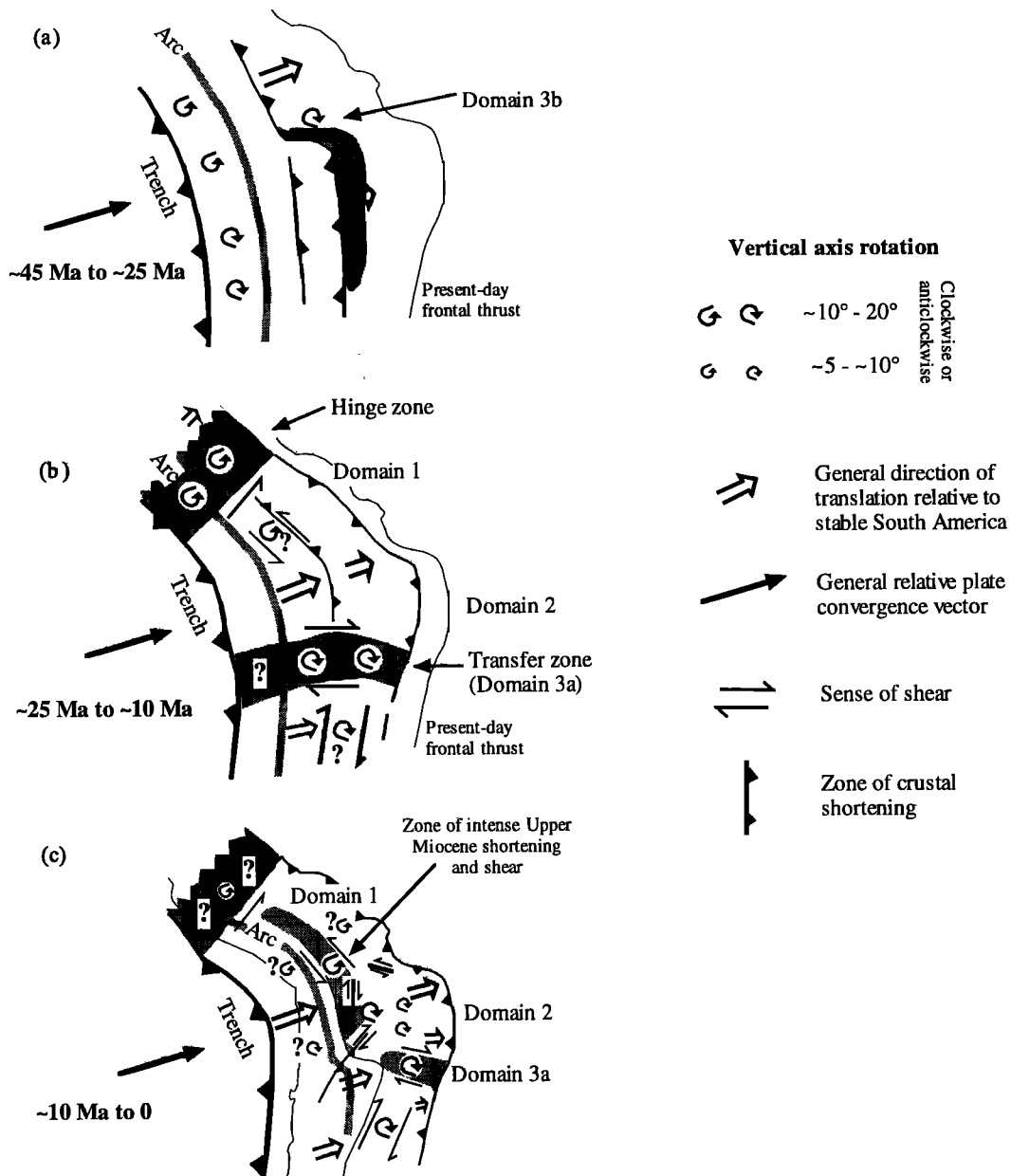


**Figure 19.** Schematic maps of the central Andes at three stages in the Cenozoic, illustrating the inferred rotational evolution of the Bolivian orocline (see text). (a) Widespread behind arc Cenozoic crustal shortening initiated in the Eocene with the development of a fold and thrust belt in what is today the western margin of the Eastern Cordillera. Margin-parallel gradients of crustal shortening here and in the forearc between ~45 Ma and ~25 Ma may have accommodated oroclinal bending of the forearc, with up to ~18° of rotation of each limb. (b) In the early Neogene, between ~25 Ma and ~10 Ma, the locus of shortening migrating eastwards toward what is today the western margin of the sub-Andean zone. This shortening appears to have accommodated translation of domains 1 and 2, without substantial bending, towards stable South America. Two transfer or hinge zones at the northern end of domain 1 and in domain 3a involved anticlockwise or clockwise internal vertical axis rotation, accommodating a reduction in the translation of regions even farther north or south. A localized zone of margin-parallel sinistral shear involving small block rotation may have been initiated in the northern Altiplano (domain 1). Margin-parallel dextral shear may have been accommodated by small block rotation, without regional bending, south of domain 3a in the Puna of northwestern Argentina. (c) In the last ~10 Myr, there has been regional rotation in domain 2, accommodated by conjugate strike-slip faulting in the Eastern Cordillera and Altiplano and along-strike gradients of shortening in the sub-Andean zone, decreasing to the south. Vertical axis rotation appears to be associated with a narrow zone of transpression in the Altiplano, both sinistral (domain 1) and dextral (domain 2). Margin-parallel dextral shear, accommodated by small block rotation, without regional bending of the western margin of the Puna of northwestern Argentina or forearc, appears to have continued south of domain 3a.

Andean zone, are not parallel to those on the western margin in the forearc of northern Chile and southern Peru (Figure 15). The swing in topographic trend is more pronounced on the eastern margin (Figure 15).

Figure 18c shows the geometric mean (with one standard deviation) of vertical axis rotations for those paleomagnetic localities within each domain which contain rocks older than ~20 Ma, plotted against the topographic trends of the eastern and western margins of the domains. The best fit line for the eastern margin plot (excluding domain 3b) has a slope less than 1 (~0.89), and, similarly, the best fit line for the western margin plot has a slope greater than 1 (~1.15) (Figure 18c).

Clearly, a plot of vertical axis rotation against the average topographic trend in the various domains would have a slope of about 1, implying a 1:1 correlation between Cenozoic vertical axis rotation and the swing in mean topographic trend around the Bolivian orocline. This correlation may be a coincidence because rotations within each domain are neither synchronous nor uniform across the width of the Bolivian orocline (see sections 5.2 and 5.3). Also, domain 3b departs significantly from this correlation (see section 5.4.1).

## 6. Evolution of the Bolivian Orocline

### 6.1. Cenozoic Crustal Strains

Unravelling the origin of vertical axis rotations in the Bolivian orocline is impossible without considering the full deformational history of Cenozoic finite crustal strains. Indeed, the spatial variation of these strains seems to require vertical axis rotation [Isacks, 1988; Beck, 1988; Kley and Monaldi, 1998; Kley, 1999].

Crustal thickening in the central Andes [James, 1971; Beck *et al.*, 1996; Wigger *et al.*, 1993], if solely a consequence of Cenozoic tectonic shortening, suggests that the total amount of shortening accommodated in the Andes decreases toward the north and south from a maximum in the hinge of the Bolivian orocline [Isacks, 1988; Kley and Monaldi, 1998; Kley, 1999]. In this case, vertical axis rotations of the western margin of the Andes relative to stable South America (anticlockwise north of the bend, clockwise farther south) would be anticipated [Isacks, 1988; Kley and Monaldi, 1998; Kley, 1999].

Balanced cross sections through the sub-Andean zone also suggest variations in the amount of tectonic shortening, from ~140 km in the bend to <70 km at ~23°S [Herail *et al.*, 1990; Baby *et al.*, 1992, 1993, 1995; Dunn *et al.*, 1995; Kley, 1999]. Given the pronounced curvilinear structural trend of the sub-Andes, one would again anticipate clockwise vertical axis rotation of the western margin of the sub-Andes and eastern margin of the Eastern Cordillera relative to stable South America, consistent with estimates of the timing and amount of shortening in the sub-Andes [Watts *et al.*, 1995; Lamb *et al.*, 1997].

The obliquity of the trend of the Andean plate margin to the average Cenozoic relative plate convergence vector between the Nazca and South American plates [Pardo-Casas and Molnar, 1987] requires components of sinistral relative plate shear north of the bend and clockwise shear south of the bend. If some of this shear is accommodated by distributed continental deformation in the Andes, then once again vertical axis rotation of small crustal blocks might be anticipated, anticlockwise north of the bend and clockwise farther south [Randall, 1998; Beck, 1998]. In addition, shortening on the eastern margin of the Andes appears to have been mainly orthogonal to the topographic trend [Lamb *et al.*, 1997; Lamb, 2000]. This requires range-parallel dextral or sinistral, possibly with associated vertical axis rotation, if translation

of the forearc, relative to stable South America has been more nearly parallel to the relative plate convergence vector [Lamb *et al.*, 1997; Lamb, 2000].

Both the variation and timing of the observed magnitude of vertical axis rotation across the width of the Bolivian orocline seem to require rotation as a consequence of all of the above mechanisms. The paleomagnetic data integrated with the tectonic evolution of the Bolivian Andes (Figure 3) [Lamb *et al.*, 1997; Lamb, 2000] suggest the following three-stage evolution of the Bolivian orocline, summarized in Figure 19.

### 6.2. Eocene to Oligocene (~45 Ma to ~25 Ma)

Paleomagnetically observed vertical axis rotation (~18° anticlockwise in domain 1) in Upper Cretaceous rocks from the forearc may record Paleogene oroclinal bending (Figure 19a) [Roperch *et al.*, 2000]. This bending, relative to stable South America, would require gradients of crustal shortening of ~30 km per 100 km along the length of the eastern margin of the Paleogene Andes, with a minimum shortening of ~100 km in the hinge zone. These amounts of shortening are difficult to account for with the observed structures in the forearc and volcanic arc alone, but could easily be accommodated by Eocene-Oligocene deformation in the Altiplano and the western margin of the Eastern Cordillera (Figure 19a) [Lamb and Hoke, 1997].

Clockwise vertical axis rotation in what is today the Cochabamba region (domain 3b), near the hinge of the Bolivian orocline, may be the result of local Paleogene deformation. One possibility is that the more northerly part of the eastern thrust front encroached on the foreland more rapidly than farther south, resulting in the formation of an oblique ramp which rotated about a vertical axis to accommodate the relative motion (Figure 19a).

### 6.3. Lower to Middle Miocene (~25 Ma to ~10 Ma)

During the Neogene, the eastern deformation front of the central Andes migrated farther east into what is today the sub-Andean zone [Lamb *et al.*, 1997]. The pattern of vertical axis rotation suggests that during the early Neogene, between ~25 Ma and ~10 Ma, the central portion of the Bolivian orocline (domains 1 and 2) translated, without substantial bending, toward stable South America, accommodated by shortening in the Eastern Cordillera and possibly what is today the western margin of the sub-Andes (Figure 19b): declination anomalies (Table 5) for localities near Arica in the Chilean forearc [Roperch *et al.*, 2000] and Salla on the western margin of the Eastern Cordillera [MacFadden *et al.*, 1990] seem to require significantly less than 10° anticlockwise regional bending during the early Neogene in the forearc and Altiplano within domain 1. This interpretation depends on assuming that the vertical axis rotations observed in ~30 Ma sandstones on the eastern limb of the Corque syncline near Chuquichambi in the northern Bolivian Altiplano (Table 5) [Roperch *et al.*, 2000] record local small block rotation and/or some of the Paleogene bending of domain 1, described above.

The northern and southern ends of the translating central portion of the orocline appear to be marked by two transfer zones or hinges, spanning the central Andes at ~15°S, north of domain 1, and at ~22°S, in domain 3a, where the crustal structure suggest marked reductions in the amount of Andean shortening (Figure 19b) [Isacks, 1988; Kley and Monaldi, 1998; Kley, 1999]. The northern zone may have acted as a hinge, decoupling regional anticlockwise Late Cenozoic rotation of central and northern Peru [Macedo-Sanchez *et al.*, 1992] from translation in domain 1. The southern zone seems to have acted as a roughly E-W dextral shear

zone (Figure 19b) with internal clockwise vertical axis rotation of crustal blocks, as well as possibly rotation of a short portion of the forearc. The significantly larger vertical axis rotation ( $\sim 35^\circ$  clockwise) observed in  $\sim 25$  Ma red beds in the sub-Andes of domain 3a, compared to that ( $\sim 19^\circ$  clockwise) in  $\sim 12$  Ma sedimentary rocks farther west, on the eastern margin of the Eastern Cordillera, suggests both clockwise vertical axis rotation and internal shortening of the western margin of the sub-Andes in domain 3a prior to the late Miocene. However, the bulk of sub-Andean shortening appears to have occurred in the last 10 Myr (see section 6.4).

Crustal shortening within the central portion of the orocline caused folding of Upper Cretaceous to Paleocene strata with sinuous axial traces. A similar local sinuosity, on a kilometer to tens of kilometer scale, can be observed in actively deforming fold and fault trends in the sub-Andean zone, especially near oblique ramps in the thrust system where displacement is transferred across strike from one thrust fault to an adjacent one. This sinuosity reflects the distribution of weak decollement horizons and is ultimately related to local facies changes in the deformed sedimentary basins. Vertical axis rotational deformation will tend to be focused at oblique ramps, amplifying the original sinuosity by sinistral or clockwise vertical axis rotation. This could have given rise to the wide scatter in paleomagnetically determined declination anomalies in Upper Cretaceous to Paleocene rocks.

#### 6.4. Upper Miocene to Present ( $\sim 10$ Ma to 0)

During the last  $\sim 10$  Myr, there has been more regional vertical axis rotation in domain 2, resulting in clockwise bending of the Eastern Cordillera and western margin of the sub-Andes in the range  $5^\circ$ - $10^\circ$ , though with possibly enhanced small block rotation, over  $10^\circ$  clockwise, in the Altiplano as a consequence of local deformation (Figure 19c). A  $\sim 7^\circ$  regional clockwise bending of domain 2 must have been accommodated relative to stable South America by a decrease in shortening of  $\sim 45$  km from north to south along the length of the sub-Andes in domain 2. The required variation in shortening is well within the estimates of shortening in this part of the sub-Andes [Herail *et al.*, 1990; Baby *et al.*, 1992, 1993, 1995; Dunn *et al.*, 1995; Kley, 1999]. All or part of this bending may also have affected the forearc in northern Chile as well.

A marked along-strike reduction in sub-Andean shortening in domain 3a, toward the south, accommodated a local  $\sim 15^\circ$  clockwise rotation of the western margin of the sub-Andes and Eastern Cordillera (Figure 19c). However, this vertical axis rotation did not extend into the Altiplano, western Puna of northernmost Argentina, or the forearc of northern Chile, suggesting an interplay between regional bending and more local deformation (Figure 19c).

Vertical axis block rotation in the eastern part of the northern Argentinian Puna may have accommodated dextral shear in a zone running parallel to the general topographic trend and bounded to the west by the undeforming and unrotating western margin of the Puna and forearc (Figure 19c). Block rotation here has been accommodated by both strike-slip faulting and thrusting, sometimes with scissor-like motions on individual thrusts [Coutand *et al.*, 1999]. A narrow, approximately NW trending (margin-parallel) zone of sinistral transpression developed on the western side of the northern Bolivian Altiplano in domain 1 (Figure 19c), possibly rejuvenating a similar zone of lower Miocene sinistral transpression. This resulted in approximately NW trending folding and thrusting [Lamb and Hoke, 1997] and  $\sim 11^\circ$  anti-

clockwise vertical axis rotation of the Corque syncline in the last 9 Myr [Roperch *et al.*, 1999].

## 7. Conclusions

This paper has presented new paleomagnetic data for the Bolivian Andes which has been used to deduce rotations about vertical axes of crustal blocks during the Cenozoic. These data, combined with previous paleomagnetic studies, have been used to constrain both the distribution and timing of rigid body rotation about a vertical axis in the Bolivian orocline.

1. The pattern of rotations is used to define three regional domains, extending across the width of the Bolivian Andes, in which blocks have undergone a regional background vertical axis rotation with superimposed local variation. The differences between the various domains is best seen in rocks in the age range  $\sim 20$  to 80 Ma. For these ages, crustal blocks in domain 1, on the northern flank of the Bolivian orocline, have undergone an anticlockwise rotation about a vertical axis in the range  $\sim 8$  to  $\sim 33^\circ$ , with a geometric mean of  $\sim 22^\circ$  anticlockwise; blocks from domain 2 immediately south of the main oroclinal bend have rotated between  $\sim 19^\circ$  anticlockwise and  $\sim 40^\circ$  clockwise, with a geometric mean of  $\sim 8^\circ$  clockwise. Even farther south, in domain 3b, blocks have rotated between  $\sim 10^\circ$  and  $\sim 57^\circ$  clockwise, with a geometric mean of  $37^\circ$ . A localized region (domain 3b) of clockwise rotations of  $\sim 32^\circ$ , in the last  $\sim 65$  Myr, is found within the southeastern part of domain 1. The northern boundary of domain 1 and the southern boundary of domain 3a are as yet not well defined. There are marked variations in both the timing and magnitude of vertical axis rotation across the width of the domains.

2. The paleomagnetic data, integrated with the evolution of tectonic shortening in the central Andes, suggest a three stage evolution of the Bolivian orocline. This may have started by oroclinal bending in the Eocene to Oligocene, accommodated relative to stable South America by margin-parallel gradients of crustal shortening in the Eocene-Oligocene fold and thrust belt on the eastern margin of the Paleogene Andes. In the lower to middle Miocene ( $\sim 25$  Ma to  $\sim 10$  Ma) shortening in and Eastern Cordillera and possibly the sub-Andean zone is inferred to have accommodated translation of the forearc and Altiplano in the central portion of the Bolivian orocline, relative to stable South America. Two transfer or hinge zones at  $\sim 15^\circ$ S and  $\sim 22^\circ$ S are associated with enhanced anticlockwise or clockwise rotation, accommodating marked reductions farther north or south in the amount of continental shortening and forearc translations. Subsequently, between  $\sim 10$  Ma and the present, shortening gradients in the sub-Andean zone accommodated  $\sim 7^\circ$  clockwise rotation of a 400 km segment of the orocline in domain 2, immediately south of the oroclinal hinge, with slightly enhance rotation farther south in domain 3a. Zones of margin-parallel sinistral or dextral shear, associated with folding and thrusting and vertical axis small block rotation developed in the Altiplano of domain 1 and the Puna/Eastern Cordillera of domain 3a, with only minor vertical rotation in the forearc or western margin of the Puna.

**Acknowledgments.** This work was carried out during the tenureship of a Royal Society Research Fellowship. Fieldwork was supported by generous grants from BP, the Royal Society, and EU. John Dewey has always been a generous source of encouragement, especially in the early stages of this work. Many people have helped me over the years, both with sampling in Bolivia and northern Chile and also with the laborious task of making paleomagnetic measurements in Oxford. I would particularly like to thank Susan Aitcheson, Brian Daniels, Jurgen Entenmann, Bryan Finnegan, Anne Grunow, Christy Hanna, Leonore Hoke, Catrin

Jones, Lorcan Kennan, Martin Shepley, Marc de Urreiztieta, Sara Vickery, Rachel Walcott, and Gerhard Woerner, who heroically helped me either in the laboratory or in trying circumstances at high altitude or in the humid lowlands of the Andes. Jim Briden and Buffy McClelland kindly gave me access to the Oxford Paleomagnetic Laboratory. Darren Randall and Conall Mac Niocaill have been sources of good advice in the latter stages of this work. The manuscript has benefitted from thorough reviews by J. Geissman and G. Taylor.

## References

- Allmendinger R., et al., The evolution of the Altiplano-Puna plateau of the central Andes, *Annu. Rev. Earth Planet. Sci.*, 25, 139-174, 1997.
- Arason, P., and S. Levi, Models of inclination shallowing during sediment compaction, *J. Geophys. Res.*, 95, 4481-4499, 1990.
- Baker, M., and P. Francis, Upper Cenozoic volcanism in the central Andes. Ages and volumes, *Earth Planet. Sci. Lett.*, 41, 175-187, 1978.
- Baby, P., G. Herail, R. Salinas, and T. Sempere, Geometry and kinematic evolution of passive roof duplexes deduced from cross-section balancing: Example from the foreland thrust system of the southern Bolivian sub-Andean Zone, *Tectonics*, 11, 523-536, 1992.
- Baby, P., B. Guillier, J. Oller, G. Herail, D. Montemurro, and M. Specht, Structural synthesis of the Bolivian sub-Andean Zone, paper presented at 3rd International Symposium, Inst. Fr. de Rech. Sci. pour Dev. en Coop (ORSTOM), Oxford, England, 1993.
- Baby, P., I. Moretti, R. Guillier, R. Limachi, E. Mendez, J. Oller, and M. Specht, Petroleum System of the Northern and Central Bolivian sub-Andean Zone, in *Petroleum Basins of South America*, edited by A. J. Tankard, R. Sutrez Suroco, and H. J. Welsink, *AAPG Mem.*, 62, 445-458, 1995.
- Beck, M., Analysis of late Jurassic-Recent paleomagnetic data from active plate margins of South America, *J. S. Am. Earth Sci.*, 1, 39-52, 1988.
- Beck, M., On the mechanism of crustal block rotations in the central Andes, *Tectonophysics*, 299, 75-92, 1998.
- Beck, S., G. Zandt, S. Myers, T. Wallace, P. Silver, and L. Drake, Crustal thickness variations in the central Andes, *Geology*, 24, 407-410, 1996.
- Beer, J.A., Steady sedimentation and lithologic completeness, Bermejo basin, Argentina, *J. Geol.*, 98, 501-517, 1990.
- Bolivian Geological Survey (GEOBOL), *1:100,000 series geological map sheets*, La Paz, Bolivia, 1962 - 1992.
- Bolivian Geological Survey (GEOBOL) and Yacimientos Petroliferos Fiscales Bolivianos (YPFB), *1:1000,000 Mapa Geologico de Bolivia*, La Paz, Bolivia, 1978.
- Butler, R.F., *Paleomagnetism: Magnetic Domains to Geologic Terranes*, Blackwell Sci., Malden, Mass., 1992.
- Butler, R., D. Richards, T. Sempere, and L. Marshall, Paleomagnetic determinations of vertical-axis tectonic rotations from Late Cretaceous and Paleocene strata of Bolivia, *Geology*, 23, 799-802, 1995.
- Coutand, I., P. Roperch, A. Chauvin, P.R. Cobbold, and P. Gautier, Vertical axis rotations across the Puna plateau (northwestern Argentina) from paleomagnetic analysis of Cretaceous and Cenozoic rocks, *J. Geophys. Res.*, 104, 22,965-22,984, 1999.
- DeMets, C., R.G. Gordon, D.F. Argus, and S. Stein, Effect of recent revisions on the geomagnetic reversal time scale on estimates of current plate motions, *Geophys. Res. Lett.*, 21, 2191-2194, 1994.
- Dewey, J.F., and S.H. Lamb, Active tectonics of the Andes, *Tectonophysics*, 205, 79-95, 1992.
- Dunn, J.F., K.G. Hartshorn, and P.W. Hartshorn, Structural styles and hydrocarbon potential of the sub-Andean thrust belt, in *Petroleum Basins of South America*, edited by A. J. Tankard, R. Sutrez Suroco, and H. J. Welsink, *AAPG Mem.*, 62, 523-544, 1995.
- Dupont-Nivet, G., P. Roperch, P. Gautier, A. Chauvin, M. Gerard, and G. Carlier, Clockwise rotations in northern Chile: Oroclinal bending or in situ tectonic rotations?, paper presented at 3rd International Symposium on Andean Geodynamics, ORSTOM, St. Malo, France, 1996.
- Evernden, J.F., S.J. Kriz, and C. Cherroni, Potassium-argon ages of some Bolivian rocks, *Econ. Geol.*, 72, 1042-1061, 1977.
- Friend, P.F., N.M. Johnson, L.E. McRae, Time-level plots and accumulation pattern of sediment sequences, *Geol. Mag.*, 126, 491-498, 1989.
- Gayet, M., L. Marshall, and T. Sempere, The Mesozoic and Palaeocene vertebrates of Bolivia and their stratigraphic context: A review, in *Fossiles y facies de Bolivia*, vol. 1, *Rev. Tec. Yacimientos Pet. Fiscales Bolivianos*, 12, 393-433, 1991.
- Gayet, M., T. Sempere, H. Cappelletta, E. Jaillard, and A. Levy, La Presence de fossiles marins dans le Cretece terminal des Andes centrales et ses consequences paleogeographiques, *Palaeogeogr. Palaeoclimatol. Palaeoecol.*, 102, 283-319, 1993.
- Grant, J.N., C. Halls, W. Avila Salinas, and N.J. Snelling, K-Ar ages of igneous rocks and mineralisation in part of the Bolivian tin belt, *Econ. Geol.*, 74, 838-851, 1979.
- Gubbels, T. L., B.L. Isacks, and E. Farrar, High-level surfaces, plateau uplift, and foreland basin development, Bolivian central Andes, *Geology*, 21, 695-698, 1993.
- Hartley, A., E. Jolly, and P. Turner, Paleomagnetic evidence for rotation in the Precordillera of northern Chile: Structural constraints and implications for the evolution of the Andean forearc, *Tectonophysics*, 205, 49-64, 1992.
- Heki, K., Y. Hamono, M. Kono, and T. Ui, Paleomagnetism of Neogene Ocos dyke swarm, the Peruvian Andes. Implication for the Bolivian orocline, *Geophys. J. R. Astron. Soc.*, 80, 527-534, 1985.
- Herail, G., et al., Structure and kinematic evolution of sub-Andean thrust system of Bolivia, paper presented at 2nd International Symposium on Andean Geodynamics, ORSTOM, Grenoble, France, 1990.
- Isacks, B., Uplift of the central Andean Plateau and bending of the Bolivian orocline, *J. Geophys. Res.*, 93, 3211-3231, 1988.
- James, D.E., Andean crustal and upper mantle structure, *J. Geophys. Res.*, 76, 3246-3271, 1971.
- Jordan, T.E., J.H. Reynolds III, and J. Erikson, Variability in age of initial shortening and uplift in the central Andes, 16°-33°30'S, in *Tectonic Uplift and Climate Change*, edited by W.F. Ruddiman, pp. 41-61, Plenum, New York, 1997.
- Kennan, L., Cenozoic tectonics of the Bolivian Andes, Ph.D. thesis, 161 pp., Univ. of Oxford, Oxford, England, 1994.
- Kennan, L., S. Lamb, and C. Rundle, K-Ar dates from the Altiplano and Cordillera Oriental of Bolivia: Implications for Cenozoic stratigraphy and tectonics, *J. S. Am. Earth Sci.*, 8, 163-186, 1995.
- Kennan, L., S. Lamb, and L. Hoke, High altitude palaeosurfaces in the Bolivian Andes: Evidence for Late Cenozoic surface uplift, in *Palaeosurfaces: Recognition, Reconstruction and Palaeoenvironmental Interpretation*, edited by M. Widdowson, *Geol. Soc., Spec. Publ.*, 120, 307-324, 1997.
- Kley, J., Geologic and geometric constraints on a kinematic model of the Bolivian orocline, *J. S. Am. Earth Sci.*, 12, 221-235, 1999.
- Kley, J., and C.R. Monaldi, Tectonic shortening and crustal thickening in the Central Andes: How good is the correlation?, *Geology*, 26, 723-726, 1998.
- Kono, M., K. Heki, Y. Hamono, Paleomagnetic study of the central Andes: counterclockwise rotation of the Peruvian block, *J. Geodyn.*, 2, 193-209, 1985.
- Kono, M., Y. Fukao, and A. Yamamoto, Mountain building in the Central Andes, *J. Geophys. Res.*, 94, 3891-3905, 1989.
- Lamb, S.H., Active deformation in the Bolivian Andes, South America, *J. Geophys. Res.*, 105, 25,627-25,653, 2000.
- Lamb, S.H., Vertical axis rotation in the Bolivian Orocline, South America, 2, Kinematic and dynamical implications, *J. Geophys. Res.*, this issue.
- Lamb, S.H., and L. Hoke, Origin of the high plateau in the Central Andes, Bolivia, South America, *Tectonics*, 16, 623-649, 1997.
- Lamb, S.H., L. Hoke, L. Kennan, and J. Dewey, The Cenozoic evolution of the Central Andes in Bolivia and northern Chile, in *Orogeny Through Time*, edited by J.-P. Burg and M. Ford, *Geol. Soc., Spec. Publ.*, 121, 237-264, 1997.
- Lavenu, A., M.G. Bonhomme, N. Vatin-Perignon, and P. De Pachtere, Neogene magmatism in the Bolivian Andes between 16°S and 18°S: Stratigraphy and K/Ar geochronology, *J. S. Am. Earth Sci.*, 2, 35-47, 1989.
- Leeder, M.R., Pedogenic carbonates and flood sediment accretion rates: a quantitative model for alluvial arid zone lithofacies, *Geol. Mag.*, 112, 257-70, 1975.
- Macedo-Sanchez, O., J. Surmont, C. Kissel, and C. Laj, New temporal constraints on the rotation of the Peruvian central Andes obtained from paleomagnetism, *Geophys. Res. Lett.*, 19, 1875-1878, 1992.
- MacFadden, B. J., F. Anaya, H. Perez, C.W. Naeser, P.K. Zentler, and K.E. Campbell, Late Cenozoic paleomagnetism and chronology of Andean basins of Bolivia: Evidence for possible oroclinal bending, *J. Geol.*, 98, 541-555, 1990.
- MacFadden, B. J., T. Sempere, and M. Gayet, The Petaca (late Oligocene-middle Miocene) and Yecua (late Miocene) Formations of the sub-Andean-Chaco Basin, Bolivia, and their tectonic significance, *Doc. Lab. Geol. Lyon Fr.*, 125, 291-301, 1993.
- MacFadden, B. J., F. Anaya, and C. Swisher III, Neogene paleomagnetism

- and oroclinal bending of the central Andes of Bolivia, *J. Geophys. Res.*, *100*, 8153-8167, 1995.
- Marshall, L.G., and T. Sempere, The Eocene to Pleistocene vertebrates of Bolivia and their stratigraphic context: A review, in *Fossiles y facies de Bolivia*, vol. 1., *Rev. Tec. Yacimientos Pet. Fiscales Bolivianos*, *12*, 631-652, 1991.
- Marshall, L.G., C. Swisher III, A. Lavenu, R. Hoffstetter, and G.H. Curtis, Geochronology of the mammal-bearing late Cenozoic on the northern Altiplano, Bolivia, *J. S. Am. Earth Sci.*, *5*, 1-19, 1992.
- McElhinny, M.W., Statistical significance of the fold test in paleomagnetism, *Geophys. J. R. Astron. Soc.*, *8*, 338-340, 1964.
- McFadden, P.L., and D.L. Jones, The fold test in paleomagnetism, *Geophys. J. R. Astron. Soc.*, *7*, 53-58, 1981.
- Pardo-Casas, F., and P. Molnar, Relative motion of the Nazca (Farallon) and South American plates since Late Cretaceous time, *Tectonics*, *6*, 233-248, 1987.
- Randall, D., A new Jurassic-Recent apparent polar wander path for South America and a review of central Andean tectonic models, *Tectonophysics*, *299*, 49-74, 1998.
- Riccardi, A., The Cretaceous system of southern South America, *Mem. Geol. Soc. Am.*, *168*, 161 pp, 1988.
- Roperch, P., and G. Carlier, Paleomagnetism of Mesozoic rocks from the central Andes of southern Peru: Importance of rotations in the development of the Bolivian orocline, *J. Geophys. Res.*, *97*, 17,233-17,249, 1992.
- Roperch, P., M. Fornari, and G. Hérail, A paleomagnetic study of the Altiplano, in *2nd International Symposium on Andean Geodynamics*, pp. 241-244, ORSTOM, Oxford, England, UK., 1993.
- Roperch, P., L. Aubry, G. Hérail, M. Fornari, and A. Chauvin, Magnetostratigraphy and paleomagnetic rotation of the North-Central Bolivian Altiplano Basin, in *3rd International Symposium on Andean Geodynamics*, pp. 477-480, ORSTOM, St. Malo, France, 1996.
- Roperch, P., G. Hérail, and M. Fornari, Magnetostratigraphy of the Miocene Corque basin, Bolivia: Implications for the geodynamic evolution of the Altiplano during the late Tertiary, *J. Geophys. Res.*, *104*, 20,415-20,429, 1999.
- Roperch, P., M. Fornari, G. Hérail, and G. V. Parraguez, Tectonic rotations within the Bolivian Altiplano: Implications for the geodynamic evolution of the central Andes during the late Tertiary, *J. Geophys. Res.*, *105*, 795-820, 2000.
- Rouchy, J.M., G. Carnoin, J. Casanova, and J.F. Deconinck, The central palaeo-Andean basin of Bolivia (Potosi area) during the late Cretaceous and early Tertiary: Reconstruction of ancient saline lakes using sedimentological, paleoecological and stable isotope records, *Palaeogeogr. Palaeoclimatol. Palaeoecol.*, *105*, 179-198, 1993.
- Sadler, P.M., Sediment accumulation rates and the completeness of stratigraphic sections, *J. Geol.*, *89*, 569-584, 1981.
- Sempere, T., Phanerozoic evolution of Bolivia and adjacent regions, in *Petroleum Basins of South America*, edited by A.J. Tankard, R. Sutrez Soruco, and H.J. Welsink, *AAPG Mem.*, *62*, 207-230, 1995.
- Sempere, T., G. Hérail, J. Oller, and M. Bonhomme, late Oligocene-early Miocene major tectonic crisis and related basins in Bolivia, *Geology*, *18*, 496-499, 1990.
- Sempere, T., R.F. Butler, D.R. Richards, L.G. Marshall, W. Sharp, and C.C. Swisher III, Stratigraphy and chronology of Upper Cretaceous - lower Palaeogene strata in Bolivia and northwest Argentina, *Bull. Geol. Soc. Am.*, *109*, 709-727, 1997.
- Somoza, R., S. Singer, and B. Coira, Paleomagnetism of upper Miocene ignimbrites at the Puna: An analysis of vertical axis rotations in the central Andes, *J. Geophys. Res.*, *101*, 11,387-11,400, 1996.
- Somoza, R., S. Singer, and A. Tomlinson, Paleomagnetic study of upper Miocene rocks from northern Chile: Implications for the origin of late Miocene-Recent tectonic rotations in the southern central Andes, *J. Geophys. Res.*, *104*, 22,923-22,936, 1999.
- Tauxe, L., and D.V. Kent, Properties of a detrital remanence carried by haematite from study of modern river deposits and laboratory redeposition experiments, *Geophys. J. R. Astron. Soc.*, *77*, 543-561, 1984.
- Torsvik, T. H., J.C. Briden, and M.A. Smethurst, *IAPD32—software for paleomagnetic analysis*, Norges Geologiske Undersøkelse (NGU), Trondheim, Norway, 1996.
- Watts, A., S. Lamb, J. Fairhead, and J.F. Dewey, Lithospheric flexure and bending of the central Andes, *Earth Planet. Sci. Lett.*, *134*, 9-21, 1995.
- Wigger, P., et al., Variation in the crustal structure of the southern central Andes deduced from seismic refraction investigations, in *Tectonics of the Southern Central Andes*, edited by K.-J. Reutter, E. Scheuber, and P. Wigger, Springer, Berlin, pp. 23-48, 1993.
- Zijderveld, J.D.A., A.C. demagnetization of rocks: Analysis of results, in *Methods in Paleomagnetism*, edited by D.W. Collinson, K.M. Creer, and S.K. Runcorn, pp. 254-286, Elsevier Sci. New York, pp 254-286, 1967.

S Lamb, Department of Earth Sciences, University of Oxford, Parks Road, Oxford OX1 3PR, England, UK. (Simon.Lamb@earth.ox.ac.uk)

(Received October 7, 1999; revised November 6, 2000; accepted November 14, 2000.)